Nanoscale Advances

REVIEW

View Article Online
View Journal | View Issue

Cite this: *Nanoscale Adv.*, 2019, **1**, 913

Biomolecule-derived quantum dots for sustainable optoelectronics

Satyapriya Bhandari, * Dibyendu Mondal, * S. K. Nataraj and R. Geetha Balakrishna

The diverse chemical functionalities and wide availability of biomolecules make them essential and cost-effective resources for the fabrication of zero-dimensional quantum dots (QDs, also known as bio-dots) with extraordinary properties, such as high photoluminescence quantum yield, tunable emission, photo and chemical stability, excellent aqueous solubility, scalability, and biocompatibility. The additional advantages of scalability, tunable optical features and presence of heteroatoms make them suitable alternatives to conventional metal-based semiconductor QDs in the field of bioimaging, biosensing, drug delivery, solar cells, photocatalysis, and light-emitting devices. Furthermore, a recent focus of the scientific community has been on QD-based sustainable optoelectronics due to the primary concern of partially mitigating the current energy demand without affecting the environment. Hence, it is noteworthy to focus on the sustainable optoelectronic applications of biomolecule-derived QDs, which have tunable optical features, biocompatibility and the scope of scalability. This review addresses the recent advances in the synthesis, properties, and optoelectronic applications of biomolecule-derived QDs (especially, carbon- and graphene-based QDs (C-QDs and G-QDs, respectively)) and discloses their merits and disadvantages, challenges and future prospects in the field of sustainable optoelectronics. In brief, the current review focuses on two major issues: (i) the advantages of two families of carbon nanomaterials (*i.e.* C-QDs and G-QDs) derived from biomolecules of various categories, for instance (a) plant extracts including fruits, flowers, leaves, seeds, peels, and vegetables; (b) simple sugars and polysaccharides; (c) different amino acids and proteins; (d) nucleic acids, bacteria and fungi; and (e)

Received 9th November 2018
Accepted 27th December 2018

DOI: 10.1039/c8na00332g

rsc.li/nanoscale-advances

Centre for Nano and Material Sciences, JAIN (Deemed to be University), Jain Global Campus, Bangalore 562112, India. E-mail: b.satyapriya@jainuniversity.ac.in; m.dibyendu@jainuniversity.ac.in; Web: dmtapu@gmail.com

Dr Satyapriya Bhandari is currently an Assistant Professor (DST-Inspire faculty) at the Centre for Nano and Material Sciences, Jain University, India. He received his Bachelor's degree (Chemistry) from The University Burdwan and Master's degree (Chemistry) from the Indian Institute of Technology (IIT), Guwahati. He received his PhD in Chemistry at IIT, Guwahati. He was a Post-doctoral Fellow at the Friedrich Alexander University, Germany, and research scientist at the Centre for Nanotechnology, IIT Guwahati. His current research interests focus on the synthesis and surface modification of quantum dots and their sustainable use in optoelectronics, solar-cells, energy conversion and environmental cleaning purposes.

Dr Dibyendu Mondal is an assistant professor at the Centre for Nano and Material Sciences (CNMS), Jain University, Bangalore, India. He received his PhD degree in 2015 in Chemical Science from CSIR-CSMCRI, Bhavnagar, India. From 2015–2017 he was a Postdoctoral Researcher at CICECO, University of Aveiro, Portugal. His main research areas focus on sustainable processes for the value addition of bioresources within the biorefinery concept. Other research activities in his group include green solvent-mediated extraction and purification and packaging of biomolecules. He is also fascinated with the design of bioinspired materials using biomacromolecules for targeted applications including, biocatalysis, water purification, energy conversion and storage.

biomasses and their waste and (ii) their applications as light-emitting diodes (LEDs), display systems, solar cells, photocatalysts and photo detectors. This review will not only bring a new paradigm towards the construction of advanced, sustainable and environment-friendly optoelectronic devices using natural resources and waste, but also provides critical insights to inspire researchers ranging from material chemists and chemical engineers to biotechnologists to search for exciting developments of this field and consequently make an advance step towards future bio-optoelectronics.

1. Introduction

Besides governing biological processes in living organisms, biomolecules, with diverse chemical functionalities and binding sites, have become sustainable precursors for the programmable, scalable and bioinspired synthesis of eco-friendly quantum dots (QDs), with superior and unique optical properties. Specifically, the new class of zero-dimensional QDs derived from biomolecules (also termed bio-dots) possesses extraordinary properties such as high photo-luminescence quantum yield and up-conversion luminescence, photo and chemical stability, excellent aqueous solubility, low cost, biocompatibility and scalability in comparison to traditional toxic metal-based QDs.[1–30] Despite their difference in crystallinity, C-QDs and G-QDs, with sizes below 10 nm, have unique common physical properties such as chemical inertness, biocompatibility, cell membrane permeability, tunable surface functional groups, water solubility and low toxicity, which are advantageous for their application in biological, optoelectronic, and energy related purposes.[1–30] Their properties make them new fluorescent nanomaterials in the family of carbon materials and superior materials in comparison to traditional organic dyes and toxic metal-based QDs. The added advantages of scalability, biocompatibility and cost-effectiveness of biomolecule-derived QDs in addition to their tunable and superior optical features make them alternative and smart choices compared to conventional semiconductor QDs for applications ranging from biodiagnostics to optoelectronics.[1–165]

Accordingly, different biomolecules such as plant extracts including fruits, seeds, peels, leaves, flowers, roots and vegetables,[31–50] sugars including monosaccharides and polysaccharides,[51–69] different amino acids and proteins,[70–89] nucleic acids, bacteria and fungi,[91–100] and biomasses and their wastes[101–121] have been used to fabricate highly luminescent QDs, especially non-metallic QDs. To date, several studies have been reported on the fabrication of biomolecule-derived eco-friendly carbon-based QDs, such as carbon QDs (C-QDs) either in their bare form or doped with hetero atoms (such as N and/or S), and graphene QDs (G-QDs), and subsequently demonstrated their excellent optical features (especially tunable emission characteristics and high quantum yield) and uses in the fields of bioimaging, drug delivery, chemical sensing, biosensing, solar-driven catalysis, and light-emitting applications.[1–121]

Over the past few decades, several synthetic techniques including top-down and bottom-up approaches have been demonstrated for the fabrication of C-QDs and G-QDs.[1–30] Top-down approaches are based on the breaking of bulk parts into smaller parts and involves methods such as solvothermal synthesis, electrochemical degradation, nanolithography, electrochemical and acidic oxidation, arc discharge, laser ablation and chemical exfoliation. In contrast, the bottom-up approach involves smaller units assembling into larger species and involves methods such as microwave irradiation, hydrothermal

Dr S. K. Nataraj is currently working as a Professor at the Centre for Nano and Material Sciences (CNMS), Jain University, Bangalore, India. He obtained his PhD in 2008 in Polymer Science from Karnatak University, Dharwad, India. Immediately after completion of his PhD, he pursued three Post-doctoral Associate assignments at Chonnam National University, South Korea (2007–2009), Institute of Atomic Molecular Sciences, Academia Sinica (2009–10), Taiwan and Cavendish Laboratory, University Cambridge, UK (2010–2013). He was awarded the DST-INSPIRE Faculty Award (2013–2015) at CSIR-CSMCRI, Bhavnagar. His main areas are the development of sustainable materials and processes for Energy and Environmental applications including water treatment.

Prof. R Geetha Balakrishna is presently the Director of the Centre for Nano and Material Sciences, Jain University, and is a core researcher on photochemistry and energy conversions in nano-materials. She currently works on perovskites, oxide/sulphide nano-crystals and colloidal quantum dots, which are active to photons and hence applicable to solar cells, water purification/disinfection/desalination and sensing technologies. She has been instrumental in developing three different Centres of research in reputed Universities. She is a Fulbright awardee for academic and professional excellence. She is a fellow/member of many renowned scientific bodies and has successfully completed many funded projects related to health, energy and water.

heating, ultra-sonication, and thermal combustion.[1–30] Interestingly, between the two approaches, the bottom up-synthesis strategy is more efficient for the synthesis of C-QDs and G-QDs considering quality, purity, cost-effectiveness and time management. Specifically, bottom-up methods yield C-QDs and G-QDs with controllable morphologies and well-distributed sizes and preserve their unique aforementioned properties, thus making them suitable for various applications.[1–30] Hence, the synthetic procedure and precursors are critical for the fabrication of excellent quality C-QDs and G-QDs for versatile applications. Earlier reports showed that some synthetic approaches such as combustion, microwave and thermal treatments of resols, citrate, polyethylene and glycol, have drawbacks in terms of costly precursors, tedious multiple steps, harsh reaction conditions (including high temperature and use of toxic solvents), use of strong acid and alkali, and purification and separation processes.[1–30] Thus, among the reported synthetic strategies, the use of biomolecules has the advantages of eco-friendliness, ease of fabrication, and scalability, and thus circumvents all the aforementioned problems related to the other bottom-up techniques. To date, different biomolecules such as (i) plant extracts including fruits, seeds, peels, leaves, flowers, roots and vegetables,[31–50] (ii) sugars including monosaccharides and polysaccharides,[51–69] (iii) different amino acids and proteins,[70–89] (iv) nucleic acids, bacteria and fungi,[91–100] and (v) biomasses and their wastes[101–121] have been utilized to synthesize biomolecule-derived carbon-based QDs. Since their discovery, biomolecule-derived C-QDs and G-QDs have been demonstrated to have extensive application potential in biological fields (imaging, drug delivery and sensing), and their use in optoelectronic devices (including LEDs, solar cells, photodetectors and supercapacitors) is quickly increasing, but yet to be explored with regard to the recent energy demand.

Thus, among all the applications of biomolecule-derived C-QDs and G-QDs, their application in optoelectronics, especially the fabrication of highly efficient sustainable optoelectronic devices (such as LEDs, display systems, solar cells, photocatalysts and photo detectors) is unique to provide new and advanced functional materials towards the development of solid-state lighting research. This may be able to reduce the global energy consumption issue, which is a long-standing problem worldwide.[2,131–165] It should be mentioned that the primary focus of optoelectronics and solid-state lighting research (especially for the fabrication of low-cost and highly efficient LEDs and solar cells) relies mainly on the sustainability and environmental friendliness of new luminescent nanomaterials.[2,131–165] The traditional approaches for the fabrication of optoelectronic devices are mostly based on the use of environmentally unfavorable materials and complicated fabrication procedures, which restrict their practical application.[2,131–165] This results in a new paradigm towards the fabrication of optoelectronic devices using natural and biological sources, which are eco-friendly in nature and have anticipated optical properties. This is where the pivotal role of biomolecule-derived C-QDs and G-QDs come into play.

There have been several reports on biomass/natural product-derived QDs (mainly C-QDs and G-QDs), which are principally focused only on their synthesis and applications in various fields, including biodiagnostics, energy conversion and catalysis.[1–165] Notably, there are ample reviews and feature articles available on the synthesis of C-QDs and G-QDs from natural products,[1,6,18] monosaccharides and polysaccharides,[21] and biomass wastes,[30] doping of heteroatoms in C-QDs and G-QDs,[22,28] applications of C-QDs in sensing,[14] bioimaging and cancer therapy,[8,15] photovoltaics and light harvesting,[23,29] synthesis, properties and various applications of G-QDs,[2,9,12,20,28] combined uses of C-QDs and G-QDs in biological purposes[10] and optoelectronic and energy applications.[2] Although vast literature exists on the application of C-QDs and G-QDs towards light-emitting applications,[131–165] to the best of our knowledge, there are no review articles on the sustainable optoelectronic applications of biomolecule-derived QDs. Hence, it is noteworthy to focus on the sustainable optoelectronic applications of biomolecule-derived QDs (more specifically C-QDs and G-QDs), which have tunable optical features, biocompatibility and scope for scalability.

The present review focuses on the use of various biomolecules for the fabrication of different luminescent QDs and their practical utilization in sustainable optoelectronics, especially LEDs, displays, solar cells, photocatalysts and photodetectors. Furthermore, this has led to the idea to sort the QDs based on the biomolecules used during their synthesis and consequently discuss their scope in certain applications. Briefly, the present review discloses two prime issues: (i) the advantages of carbon- and graphene-based QDs (C-QDs and G-QDs) derived from biomolecules of various categories and (ii) their applications as LEDs, display systems, solar cells, photocatalysts and photo detectors. Overall, the present review uncovers a brief conceptual idea and novel insights into how biomolecule-derived QDs can be used to construct sustainable optoelectronic devices, followed by overcoming the existing problems. Fig. 1 clearly depicts the use of different biomolecules towards the fabrication of biomolecule-derived QDs with extraordinary properties and their subsequent importance in various optoelectronic applications.

2. Biomolecule-derived quantum dots (QDs)

Realizing the importance of biomolecule-derived QDs, the present section is systematically divided into sub-sections based on the use of different biomolecules towards the fabrication of QDs. Specifically, the different QDs are grouped based on the classification of the biomolecules used during their synthesis. The synthetic procedure, optical properties and applications, especially disclosing the scope of their use as sustainable optoelectronic materials based on their optical features, of biomolecule-derived QDs are clearly described herein. Importantly, natural products (biomolecules) can be used to prepare scalable, biocompatible and highly luminescent C-QDs and G-QDs *via* methods that are more cost-effective, greener and simpler than the traditional methods using man-made carbon-based sources.[1] To date, different biomolecules

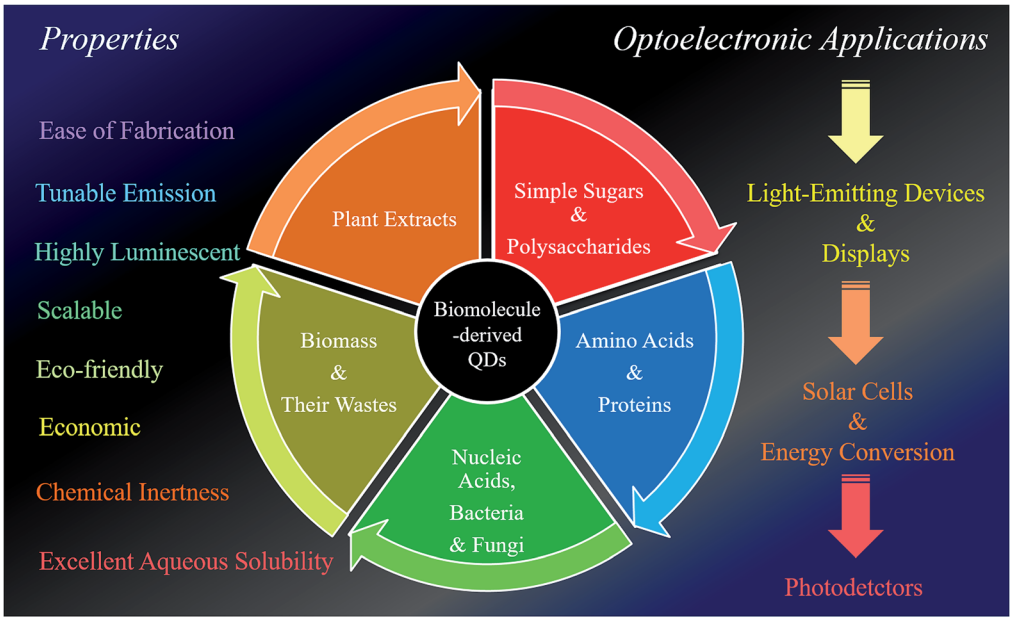

Fig. 1 Schematic illustration of the natural synthetic precursors of biomolecule-derived QDs, and their extraordinary properties and use in different optoelectronic applications.

such as (i) plant extracts including fruits (apples, oranges, mangos, bananas, *etc.*), seeds (grape and lychee), peels (water melon and pineapple), leaves (plane, lotus, ginkgo, pine, osmanthus, palm, camphor, maple and bamboo, and tea), flowers (rose), roots (lotus), and vegetables (cabbage, potato, tomato, curcumin, *etc.*),[31–50] (ii) sugars including monosaccharides (glucose, fructose, galactose, *etc.*) and polysaccharides (chitosan, alginic acid, cellulose, starch, glycogen, chitin and starch),[51–69] (iii) different amino acids (glycine, histidine, cystine, cysteine, serine, glutamic acids, isoleucine, *etc.*) and proteins (bovine serum albumin (BSA), hemoglobin, β-lactoglobulin, *etc.*),[70–89] (iv) nucleic acids (deoxyribonucleic acid (DNA)), bacteria (*Escherichia coli* (*E. coli*), *Staphylococcus aureus* (*S. aureus*), harmful cyanobacteria) and fungi (mushrooms),[91–100] and (v) biomasses (rice husk, coffee grounds, plant leaves, wood charcoal, grass, sugarcane molasses, bird feathers and eggs, bakery products, human hair and nails, soybean oil, coconut shells, *etc.*) and their wastes (food/agricultural waste containing carbohydrates, cellulose, chitin, lignin, chitosan, inorganics, hemicelluloses, lignin, proteins, *etc.*)[101–121] have been used to fabricate highly luminescent biomolecule-derived carbon-based QDs, especially non-metallic QDs. To date, several studies have been reported on the fabrication of biomolecule-derived eco-friendly carbon-based QDs, such as C-QDs either as their bare form or doped with hetero atoms (such as N and/or S) and G-QDs, and subsequently demonstrated their excellent optical features (especially tunable emission characteristics and high quantum yield) and uses, mostly in the fields of bioimaging, drug delivery, chemical sensing, biosensing, solar driven catalysis, and light-emitting applications. Therefore, based on the classification of the biomolecules generally used during the synthesis of C-QDs and G-QDs, this part of the review is divided into sub-sections as follows.

2.1. QDs from plant extracts

Plant extract-derived biodots are renewable, cost-effective and eco-friendly, and the presence of heteroatoms is beneficial for the construction of heteroatom-doped bio-dots without the use of additional sources of heteroatom-containing species.[1,31–50] Plant extracts have been demonstrated to be exceptional sources for the green fabrication of biodots, especially C-QDs and G-QDs, since they are rich carbon-containing species.[1,31–50] Plant extract-derived QDs have shown tremendous physical features including high photoluminescence quantum yield (QY), photostability, excellent water solubility and lower cytotoxicity compared to ordinary dye and metal-based QDs, and thus demonstrated application potential in bioimaging, biosensing, photocatalysis and optoelectronics.[1,2,31–50] Furthermore, plant extracts such as vegetables, fruits, flowers, leaves, seeds, roots and peels have already proven to be outstanding and alternative carbon precursors for the fabrication of C-QDs and G-QDs, and thus demonstrated their uses in many of the aforementioned fields. Fruit juices (orange, banana, apple, papaya, pear, *etc.*) have been employed as carbon sources for the fabrication of highly luminescent water soluble nontoxic biodots. For example, (i) orange juice, following hydrothermal treatment, was used to fabricate highly green luminescent photostable and nontoxic C-QDs with a QY of 26%, which were used as a cellular imaging agent (Fig. 2A).[31] (ii) Water-soluble green luminescent C-QDs with a QY of 8.95% and pH-dependent luminescence properties were synthesized based on the simple heating of banana juice without the use of any surface passivation agents.[32] (iii) The hydrothermal treatment of apple juice was used to construct bright-blue fluorescent monodispersed nontoxic C-QDs (having a QY of 4.27%), which were subsequently used as a fluorescent probe for the imaging of

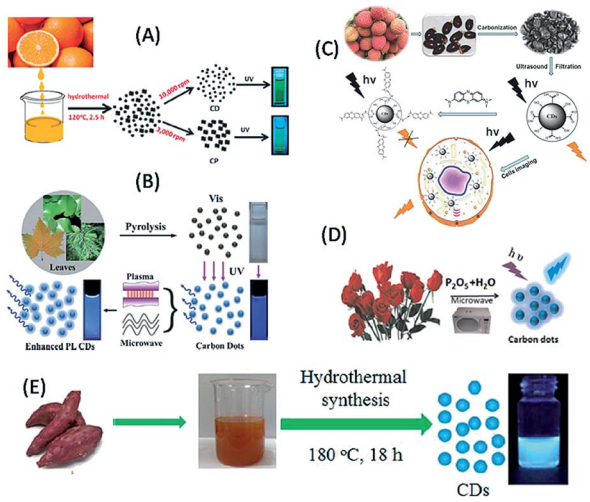

Fig. 2 Fabrication of biomolecule-derived QDs using different plant extracts as a source of carbon. (A) Orange juice (this figure has been adapted/reproduced from ref. 31 with permission from The Royal Society of Chemistry), (B) lychee seeds (this figure has been adapted/reproduced from ref. 37 with permission from The Royal Society of Chemistry), (C) plane, lotus, pine leaves (this figure has been adapted/reproduced from ref. 42 with permission from The Royal Society of Chemistry), (D) rose flower (this figure has been adapted/reproduced from ref. 45 with permission from Elsevier) and (E) sweet potato (this figure has been adapted/reproduced from ref. 47 with permission from Elsevier).

mycobacterium and fungal cells.[33] (iv) Carica papaya juice, followed by hydrothermal treatment, was used as a carbon precursor to synthesize blue luminescent biocompatible C-QDs, with a QY of 7%, which were used as cellular imaging agents for bacterial (*Bacillus subtilis*) and fungal (*Aspergillus aculeatus*) cells.[34] (v) Similarly, a C-QD-based weak gel from pear juice, with excitation dependent multicolour emissions, was also reported and used for sensing purposes.[35]

Seeds have also used to synthesize biodots (including C-QDs and G-QDs). For example, (i) the microwave-assisted synthesis of self-assembled G-QDs (with a QY of 31.79% and excitation-dependent luminescence) from grape seed extract was reported, which were used in nucleus targeting in theranostics, organelle labelling, and optical pH sensing probes.[36] (ii) Lychee seeds, following pyrolysis, served as a carbon source for the synthesis of blue luminescent C-QDs with a QY of 10.6% (Fig. 2B), and subsequently used as sensor for methylene blue and as a bioimaging agent in living cells.[37] Peels of fruits have also been used to construct water-soluble and highly luminescent biodots. For example, (i) the low temperature carbonization of water melon peel was used to synthesize blue luminescent, stable, water-soluble, nontoxic C-QDs with a QY of 7.1%, which were used as a cellular imaging agent.[38] (ii) Pineapple peel served as a carbon source for the synthesis of strong blue luminescent, low cytotoxic C-QDs with a QY of 42%, which were subsequently used in the sensing of heavy metal ions, imaging of cancerous HeLa cells, and fabrication of electronic logic gates.[39] (iii) Orange peels were used to fabricate highly blue luminescent C-QDs, having a QY of 36% *via* hydrothermal carbonization, which showed photocatalytic activities in combination with ZnO for the degradation of an azo dye.[40] (iv) Similarly, pomelo peel served as a carbon source for the hydrothermal-based synthesis of water-soluble, highly blue fluorescent C-QDs with a QY of 6.9%, which were used for the detection of heavy metal ions.[41] Leaves of plants have also been used for the large-scale production of high quality biodots without the use of any surface passivation agent or toxic/expensive solvents. For example, leaves from plane, lotus and pine were used for the one-pot pyrolytic synthesis of low-cost, biocompatible, blue luminescent C-QDs, with excitation tunable fluorescence and QYs of 16.4, 15.3 and 11.8, respectively (Fig. 2C). Consequently, the formed C-QDs acted as a sensor for the detection of Fe^{3+} ions, luminescent inks for printing luminescent patterns and used to fabricate fluorescent micro-beads, followed by their encapsulation in polymers, which may be useful for future biodiagnostic applications.[42] Similarly, tea including their leaves and powder forms, was used to fabricate blue luminescent C-QDs with excitation tunable emission properties and conductive fabrics.[43] Notably, the roots of plants (such as the lotus) have also been used as a carbon source for the microwave-assisted fabrication of blue luminescent N-doped C-QDs with a QY of 19% and in heavy metal ion sensing and multicolour cellular imaging.[44] Besides the fruits, the seeds, peels, leaves and roots of plants and their flowers, for example the rose plant, were used as a carbon source for the synthesis of C-QDs, which exhibited blue emission, QY of 13.45%, and excitation-dependent emission properties (Fig. 2D), and consequently application in the analytical sensing of tetracycline.[45] Similarly, vegetables such as cabbage, potato, capsicum, curcumin and tomato have been used as a renewable source of carbon to synthesize biodots with excellent properties and desired applications. For example, (i) Kim and co-workers reported the low temperature carbonization of cabbage for the production of highly blue luminescent nontoxic C-QDs with a QY of 16.5% and excitation-dependent emissive properties, which had served as a bioimaging agent.[46] (ii) Sweet potato was used for the synthesis of blue luminescent N-doped C-QDs with a QY of 8.64% *via* a hydrothermal reaction, (Fig. 2E), which were used to probe Fe^{3+} in living cells.[47] (iv) The microwave-assisted pyrolysis of tomato in the presence of ethylene diamine (EDA) and urea resulted in the formation of nontoxic blue fluorescent C-QDs (with 1.77% QY), which exhibited excitation-tunable fluorescence properties and were used for the bioimaging of plant pathogenic fungi and the detection of vanillin.[48] (iv) Packirisamy and co-workers demonstrated the use of curcumin as a source of carbon for the hydrothermal-based synthesis of blue luminescent C-QDs, with high aqueous solubility, QY of 8.607% and efficient excitation-dependent multicolour fluorescent emission, which were useful in bioimaging and sensing purposes.[49] Notably, Wang *et al.* reported the use of a series of vegetables, including guava, red pepper, peas and spinach, as a carbon precursor for the synthesis of blue luminescent C-QDs and eventually revealed that the spinach-extracted C-QDs exhibited higher luminescence properties among the utilized vegetables.[50] Interestingly, the coupling of spinach-derived blue luminescent C-QDs with TiO_2 resulted in enhanced

photocatalytic activities for hydrogen generation.[50] Hence, the various parts of plants have been demonstrated for the construction of biodots (mostly C-QDs) in green and cost-effective pathways, which have various uses, especially in bio-imaging and sensing activities.

2.2. QDs from simple sugars and polysaccharides

The smallest carbohydrates with low molecular weights are known sugars (including mono and disaccharides), where oligomeric and polymeric units of monosaccharides lead to the formation of oligo and polysaccharides, which are two other classes of carbohydrates.[21,51–57] Sugars and polysaccharides include numerous important molecules that play vital roles in fertilization, the immune system, storing energy, and preventing blood clotting and pathogenesis, and thus are important for living organisms.[21,51–57] The diverse functionalities, availability, abundance, heterogeneity, high water solubility, low carbonization temperatures, low cost and lack of toxicity of sugars and polysaccharides make them important class of biomolecules, which can be used as starting materials for the construction of highly luminescent, biocompatible and low cost QDs (including C-QDs and G-QDs).[21,51–57] Thus, researchers have started to use sugars and polysaccharides as carbon sources to construct C-QDs and G-QDs, with enhanced and superior physical and optical properties. To date, simple sugars such as glucose, fructose, sucrose, glucosamine, mannose, maltose and lactose and their derivatives have been used for the synthesis of biomolecule-derived QDs.[21,51–69] Similarly, polysaccharides such as chitosan, cellulose, starch, glycogen, dextran, hyaluronic acid, and chitin have also been successfully used to synthesize biodots, with control over their optical and physical properties.[21,58–69] Among the monosaccharides, glucose has been extensively been used in the synthesis of C-QDs.[51–57] For example, (i) Peng *et al.* demonstrated the synthesis of highly blue luminescent nontoxic C-QDs, with a QY of 13% using glucose as a carbon source followed by acid treatment and surface passivation with 4,7,10-trioxa-1,13-tridecanediamine (TTDDA).[51] (ii) Yang *et al.* reported the formation of highly water-soluble C-QDs with blue luminescence and QY of 6.3% *via* microwave-assisted synthesis using glucose as a carbon source in the presence of poly(ethylene glycol)-200 (PEG-200) (Fig. 3A).[52] (iii) Glucose-derived water soluble G-QDs with a QY in the range of 7–11% were synthesized *via* microwave-assisted synthesis, which were used to fabricate a white-light emitting material based on their coating on a blue LED chip.[53] (iv) Blue luminescent (N, P) dual-doped C-QDs with a 30% QY were synthesized *via* the hydrothermal treatment of glucose in the presence of ammonia and phosphoric acid, which were used for the imaging of cells and detection of Fe^{3+} ions.[54] (v) Similarly, green emissive glucose-derived C-QDs with a QY of 9.6% were synthesized and demonstrated to be an ideal candidate as a better bioimaging agent compared to blue luminescent C-QDs.[55] Besides the use of glucose, other monosaccharides such as fructose, maltose and sucrose and their derivatives such as polyols (glycerol and xylitol) and glucosamine hydrochloride have also been used as carbon sources for the fabrication of C-QDs. For example, (i) a combination of maltose and fructose (in the presence of bases) was used as a carbon source for the room temperature fabrication of green luminescent and highly crystalline C-QDs (with s QY 2.2%).[58] (ii) Phosphoric acid was reported to facilitate the synthesis of orange-red luminous C-QDs with a QY of 15% from sucrose (Fig. 3B).[59] (iii) The microwave irradiation of glucosamine hydrochloride in the presence of TTDDA resulted in the formation of blue-emitting C-QDs with a QY of 17%.[60] (iv) The microwave irradiation- and TTDDA facilitated-pyrolysis of glycerol resulted in the formation of blue luminescent C-QDs with a QY of 12%, which were used for live cell imaging.[61] (v) Xylitol in the presence of acids and ethylene diamine was used as a carbon source for the fabrication of blue fluorescent nontoxic photostable C-QDs (with 7% QY), which were subsequently used for the imaging of cancerous HeLa cells.[62]

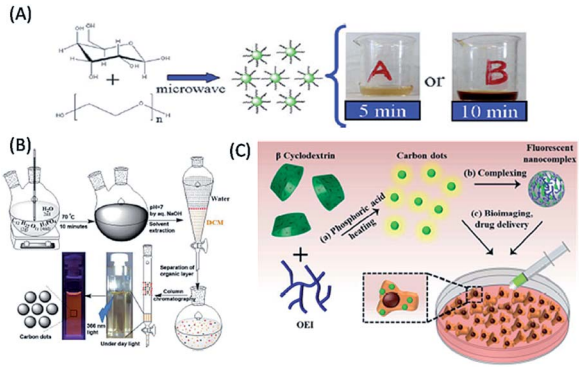

Fig. 3 Synthesis of biomolecule-derived QDs based on the use of different carbohydrates and their derivatives as carbon precursors. (A) Glucose (this figure has been adapted/reproduced from ref. 52 with permission from The Royal Society of Chemistry), (B) sucrose (this figure has been adapted/reproduced from ref. 59 with permission the PCCP Owner Societies), and (C) β-cyclodextrin (this figure has been adapted/reproduced from ref. 68 with permission from The Royal Society of Chemistry).

Also, polymeric sugar molecules, also termed polysaccharides, such as chitin, chitosan, cellulose, hyaluronic acid, and cyclodextrin, are important precursors for the fabrication of biomolecule-derived QDs. Hydrothermal treatment of chitin, which is composed of β-1,4-linked *N*-acetyl-D-glucosamine units, in the presence of acids resulted in the formation of blue luminescent N-doped C-QDs.[63] Chitosan (an amine-containing polysaccharide) hydrogel-derived blue luminescent C-QDs were synthesized *via* microwave irradiation in the presence of acid and glycerol, which were subsequently used to fabricate pH-responsive drug-delivery vehicles based on their coating of calcium alginate (CA) beads.[64] Similarly, the microwave irradiation of chitosan, alginic acid and starch individually in the presence of PEG-200 led to the formation of blue luminescent spherical C-QDs with different luminescence intensities and QYs.[65] Among them, the starch-based C-QDs showed the highest luminescence properties and were an efficient sensing platform for Cu^{2+} ions.[65] Notably, cellulose, a linear polysaccharide composed of repeating β-1,4-linked glucose units, was used to synthesize blue-green emissive C-QDs with a QY of

21.7% and the ability to image cells.[66] Additionally, the cyclic glucose polymer cyclodextrin has been used as a carbon precursor for the synthesis of C-QDs (with a QY of 13.5%) *via* acidic and hydrothermal treatment, which exhibited excitation-dependent emissive behaviour and potential in sensing of Ag^+ ions.[67] The thermolysis of the β form of cyclodextrin (*i.e.*, β-cyclodextrin) in presence of surface passivation agents and acid has been used to construct excitation-independent green emissive photostable C-QDs (with a QY of 30%, Fig. 3C), which were coupled with a negatively-charged polysaccharide (hyaluronic acid) for drug delivery applications.[68] Similarly, an N-containing polysaccharide, hyaluronic acid, served as a starting material in combination with glycine (followed by autoclave treatment) for the synthesis of C-QDs with excitation-dependent fluorescence from the blue to green emission window, which were consequently used as a fluorescent probe for targeted live cell labelling, imaging and drug delivery applications.[69] The above discussion reveals the extensive use of carbohydrates, including simple sugars (mono and disaccharides) and polysaccharides as cheap and easily available starting carbon materials for the fabrication of nontoxic, highly water-soluble, highly luminescent C-QDs, which have significant impact in biological imaging, sensing and drug delivery applications.

2.3. QDs from amino acids and proteins

Amino acids, the elementary structural units of proteins, are abundant, eco-friendly, cheap and biocompatible. The presence of the different functional groups, especially both amino and carboxyl groups, makes them excellent molecular precursors for the programmable bioinspired synthesis of biomolecule-derived QDs (biodots) with anticipated properties.[70–83] Interestingly, the abundant nitrogen- and sulphur-containing functional groups in amino acids provide the additional advantage of heteroatom doping biomolecule-derived QDs (particularly in C-QDs and G-QDs), which results in better crystallinity and extraordinary optical properties.[70–83] Moreover, owing to their highly versatile combinations of different functional groups, amino acids offer greater programmability towards the construction of high quality biomolecule-derived QDs. For example, C-QDs were synthesized *via* the microwave irradiation of histidine in the presence of acid/alkali, which exhibited strong blue fluorescence (with a QY of 44.9%) and enhanced chemiluminescence in the presence of a sodium periodate-hydrogen peroxide system.[70] Whereas, hydrothermal treatment of histidine in the presence of acid/alkali resulted in the formation of highly blue luminescent, nontoxic, photostable N-doped C-QDs with a QY of 8.9% and excitation tunable luminescence behaviour, which were used as a sensor for Fe^{3+} ions and imaging agent for cancerous cells (Fig. 4A).[71] Recently, 20 different natural α-amino acids and their mixtures were used to fabricate highly photostable C-QDs (with a QY of 30.44%), which demonstrated that the reactive R groups present in amino acids determine the stability of surface defects, morphology, crystallinity and optical features of amino acid-derived C-QDs.[72] Similarly, L-serine and L-cystine were used to synthesize (N, S) co-doped C-QDs, which were utilized in

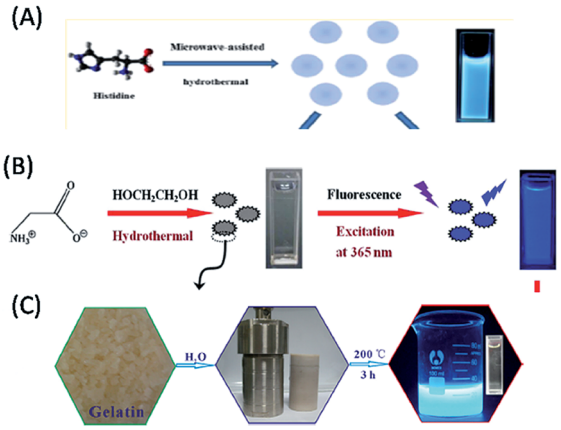

Fig. 4 Construction of biomolecule-derived QDs with the use of different amino acids and proteins as carbon sources. (A) Histidine (reproduced from ref. 71 with permission from the American Chemical Society), (B) glycine (reproduced from ref. 80 with permission from Springer Nature), and (C) gelatin (reproduced from ref. 89 with permission from The Royal Society of Chemistry).

bioimaging applications.[73] Similarly, L-aspartic acid in the presence of glucose was exploited as a carbon source for the synthesis of biocompatible C-QDs with full-colour tunable emission (465–550 nm) and high QY of 7.5%, which served as fluorescence imaging and targeting agents for non-invasive glioma diagnosis.[74] Cysteine was also used for the synthesis of highly luminescent water-soluble C-QDs (with a maximum QY of 38%), which were subsequently demonstrated to have applications in numerous fields, such as label-free sensing of Cd^{2+}/Fe^{3+}, *in vitro* imaging of MCF7 cancer cells, anti-bacterial activity against *Escherichia coli* (*E. coli*), and photocatalytic activity towards H_2O_2.[75] Lysine-derived blue luminescent chiral C-QDs *via* thermal treatment of D- or L-lysine (Lys) as the solitary carbonaceous building block showed chiral inhibition of the assembly and fibrillation of the prion peptide.[76] Similarly, the hydrothermal treatment of isoleucine in the presence of citric acid was used to construct blue luminescent, water-soluble, N-doped C-QDs, which acted as a turn-off fluorescent probe for the detection of Fe^{3+} in aqueous solution.[77] In addition, glutamic acid was also used as a precursor for the synthesis of C-QDs, with a QY of 30.7% and excitation tunable luminescence, which were used as an imaging agent for plant cells.[78] Interestingly, the pyrolysis of L-glutamic acid resulted in the formation of stable and biocompatible G-QDs with a high QY (54.5%) and strong excitation-dependent photoluminescence including near-infrared (NIR) fluorescence in the range of 800–850 nm (depending on the excitation wavelength), which were consequently used as a biomarker for *in vitro*/*in vivo* imaging and sensor for hydrogen peroxide.[79] Whereas, highly luminescent blue-emitting nitrogen-doped and amino acid-functionalized G-QDs (with a QY of 16.2%) were prepared using glycine as a precursor (Fig. 4B), which were used for the fluorometric determination of ferric ions.[80]

Proteins are natural bio-macromolecules rich in various functional groups at defined locations of the main chain of

peptide bonds and can easily unfold into peptide polymers, depending on reaction and environmental conditions.[81–89] These different functional groups in a single entity make proteins an excellent source of ligands, ranging from thiols and carboxylate to amine moieties. Thus, they are not only used as templates (or stabilizing agents) for the synthesis of various metal-based traditional QDs, but also to help to modify the surface of pre-synthesized hydrophobic QDs and make them biologically amenable for overcoming their restricted biological applications.[81–89] Since the 21st century, proteins, including their denatured forms, have been used as carbon sources for the fabrication of biomolecule-derived QDs (especially, C-QDs).[81–89] In this regard, bovine serum albumin (BSA), β-lactoglobulin, hemoglobin and gelatin have been demonstrated as protein sources for the construction of biocompatible, highly luminescent biomolecule-derived QDs.[81–89] Among them, BSA (both in its normal and denatured forms) has efficiently utilized as a facile and green synthetic precursor for the synthesis of C-QDs. For example, (i) the hydrothermal treatment of BSA in the presence of a surface passivating agent resulted the formation of low-cytotoxic, biocompatible and highly blue luminescent C-QDs, which were useful for cellular imaging applications.[81] (ii) The carbonization of BSA (in hot water) led to the formation of good quality C-QDs with a high QY of 34.8%, narrow size distribution, colloidal stability in a wide pH range and high salt concentration, and excitation-dependent tunable fluorescence in the range of 450–525 nm, which subsequently exhibited versatility in single particle dynamic imaging and Fe^{3+} ion sensing in spring water.[82] (iii) Microwave treatment of the denatured form of BSA was used to fabricate blue luminescent C-QDs with a QY of 14% and up-conversion fluorescence properties, which served as a nanosensor for pH, temperature and silver metal ions.[83] In addition, the hydrothermal reaction of BSA (in water) resulted in the formation of highly fluorescent N-doped C-QDs, with a QY of 44% and excitation-dependent emission behaviour, which were consequently used as an imaging probe for live mammalian cells.[84] Furthermore, highly blue fluorescent, biocompatible, N doped C-QDs (with a QY of 17.1%) were fabricated *via* the hydrothermal treatment of BSA (together with formic acid), which were consequently used for live cell nuclear-targeted imaging.[85] Interestingly, a drug delivery system containing hollow, blue luminescent, stable, nontoxic C-QDs (with a QY of 7%) was fabricated *via* a solvothermal reaction using BSA as the carbon source.[86] Similarly, β-lactoglobulin, which is less hydrophobic, smaller, and highly resistant to proteolytic degradation than BSA, was used to construct highly blue luminescent C-QDs with excitation-independent emission, which subsequently served as a sensing platform for the detection of Cu^{2+} ions.[87] Recently, the hemoglobin molecule, which consists of a heme group (with an Fe^{2+} ion bound within a porphyrin ring) and four globular protein subunits, was used to synthesize blue luminescent C-QDs (also termed blood dots: containing Fe^{2+} ions), which were used as a sensor for hydrogen peroxide.[88] Similarly, gelatin was used as a protein source for the synthesis of blue luminescent C-QDs, with a QY of 31.6% and excitation-dependent, up-conversion and pH-sensitive luminescence properties, which were used as an excellent fluorescent ink material and bioimaging agent (Fig. 4C).[89] Therefore, the above discussion clearly demonstrates that amino acids and proteins have been used to construct fluorescent, eco-friendly, highly luminescent C-QDs and G-QDs, which have been used typically for bioimaging, drug delivery and/or sensing applications.

2.4. QDs from nucleic acids, fungus and bacteria

Nucleic acids are natural biopolymers of nucleotides, which consist of three components: nitrogenous nucleobases (purine and pyrimidine), phosphate group and pentose sugar. The difference in the structure of the pentose sugars (in the nucleotides) and the presence of different nucleobases (in addition to three common nucleobases, adenine, cytosine and guanine) have been used to classify nucleic acids into two categories: RNA, which contains ribose (with hydroxyl groups) as the sugar and uracil as the nucleobase, while DNA contains 2-deoxyribose as the sugar and thymine as the nucleobase.[90–94] The presence of the different chemical moieties in nucleic acids make them important biological molecules towards the functionalization and stabilization of different QDs.[91–94] Over the last decade, nucleic acids (especially DNA) have been demonstrated as starting carbon source materials for the synthesis of biomolecule-derived QDs (mostly C-QDs).[91–94] For example, (i) Guo *et al.* reported that the cytosine-rich DNA (obtained from salmon testes or salmon sperm DNA) was used as a carbon source to synthesize blue fluorescent biomolecule-derived QDs *via* self-assembly at low temperature, with excellent solubility, low cytotoxicity, stable blue fluorescence (with a QY of 3.65%) and good biocompatibility.[91] (ii) Inspired by this, Qiu and co-workers also demonstrated the hydrothermal treatment of polycytosine DNA (at low temperature) for the fabrication of blue luminescent bio-dots, which, after subsequent combination with Ag^{+} ions, were used for the detection of biothiols and glutathione reductase activity.[92] (iii) DNA-derived blue luminescent C-QDs were also prepared *via* the hydrothermal treatment of DNA, which were efficiently used for the detection of mercury and silver ions in water (Fig. 5A).[93] (iv) Finally, bacterial genomic DNA (isolated from *Escherichia coli*) was demonstrated as a starting material for the synthesis of highly fluorescent, biocompatible C-QDs and the presence of ample chemical groups, including amino or hydroxyl groups made them a useful platform for cellular imaging for both prokaryotic and eukaryotic cells as well as drug delivery agents in organelles and cells.[94]

Microorganisms such as fungi, (multicellular eukaryotic organisms have nuclei contacting chromosomes and other organelles) and bacteria, (single-celled prokaryotes without nuclei and smaller in size compared to fungi) have recently been used as carbon sources for the green synthesis of highly fluorescent, low cost biomolecular QDs (mostly C-QDs), and thus applicability in fields ranging from bioimaging and sensing to drug delivery.[95–99] Recently, edible mushrooms (*Pleurotus* spp. fungus) were used to synthesize blue luminescent and water-soluble C-QDs with a QY of 25%, which were used as a fluorescent probe for the label-free detection of Hg^{2+}

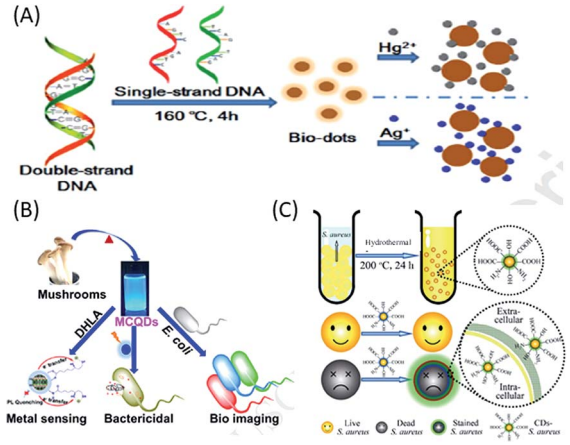

Fig. 5 Use of (A) nucleic acid (DNA), (B) fungus (mushroom) and (C) bacteria (*S. aureus* or *E. coli*) as a carbon sources to synthesize biomolecule-derived QDs. (A) has been adapted/reproduced from ref. 93 with permission from Elsevier, (B) from ref. 95 with permission from Elsevier, and (C) from ref. 97 with permission from The Royal Society of Chemistry.

ions, photo-induced bactericidal agent and for the labelling of bacteria (Fig. 5B).[95] Additionally, blue luminescent C-QDs, with a QY of 15.3% QY, excellent photostability and nontoxicity, were synthesized *via* the one-step hydrothermal treatment of a fungus (mushroom) for a short period of time, which were used for sensing hyaluronic acid and hyaluronidase.[96] On the other hand, using different bacteria, application-specific C-QDs have been constructed. For example, (i) *Staphylococcus aureus* (*S. aureus*) and *Escherichia coli* (*E. coli*) bacteria were used to synthesize low-cost eco-friendly and scalable C-QDs *via* hydrothermal carbonization, with high photostability and excitation-tunable luminescence, which were used to rapidly distinguish dead microorganisms from live ones (Fig. 5C).[97] (ii) Harmful cyanobacteria, which seriously impact humans and the ecosystem, were successfully converted into highly luminescent, photostable, uniform and low-cytotoxic C-QDs, which were used as an efficient imaging (carbon nanotags) platform for anti-cancer therapy, and is a step towards sustainability and economic benefit.[98] (iii) Using *L. plantarum*, as a single carbon source, highly fluorescent C-QDs with a QY of 10.3% were fabricated, which, importantly, exhibited properties to inhibit biofilm formation of *Escherichia coli* without affecting cellular growth.[99] Thus, the above conversation evidently shows that nucleic acids, fungi and bacteria can be successfully used as a carbon sources for the synthesis of biodots (mainly C-QDs), which have applications in various biological fields, including imaging, drug delivery, and sensing.

2.5. QDs from biomass and their waste

Realizing the need for cheap, renewable, abundant and eco-friendly carbon sources for the synthesis of biomolecule-derived QDs (including C-QDs and G-QDs), biomass and their wastes have recently received great attention, and thus far served well to fulfil the requirements for their synthesis. In this regard, various biomass and their wastes, for example, (i) agricultural products,[100–107] (ii) animals and their derivatives,[108–112] (iii) foods (including bakery products and beverages),[113–119] and (iv) industrial products,[120,121] have been demonstrated to be applicable for the scalable, low-cost synthesis of carbon-based QDs, with superior optical features and applications mostly in biological and sensing purposes.

Agricultural products and their wastes, such as rice husk, sugar cane molasses and bagasse, chia seeds, coffee grounds, grass, dead neem leaves, and wood charcoal, have been used as carbon precursors for the fabrication of application-specific C-QDs and G-QDs.[100–107] For example, Wang *et al.* reported the use of rice husk as an abundant source of biomass for the large-scale and hydrothermal-based synthesis of biocompatible blue luminescent G-QDs with a QY of 8.1%, excellent water solubility, stability and tunable luminescence properties, and subsequently demonstrated their use in cellular imaging (Fig. 6A).[100] Huang *et al.* reported the formation of biocompatible blue luminescent C-QDs (having a QY of 5.8%) based on the thermal treatment of sugarcane molasses (as the carbon source), which were used as bioimaging agents and sensor for Sunset Yellow.[101] Du *et al.* reported the renewable waste of bagasse could also be useful as a raw material for the fabrication of highly luminescent photostable biocompatible C-QDs with excitation tunable emission in the blue, green and red emission windows and potential as a bioimaging agent.[102] Jones *et al.* reported that the thermal treatment of chia seed, a renewable natural biomass, resulted in the formation of amorphous scalable C-QDs, with a QY in the range of 4–25% and multicolor luminescence properties in different solvents.[103] Chang and co-workers reported the use of coffee grounds as a carbon raw material source, for the green, low cost and scalable synthesis (using simple heating) of nontoxic C-QDs with

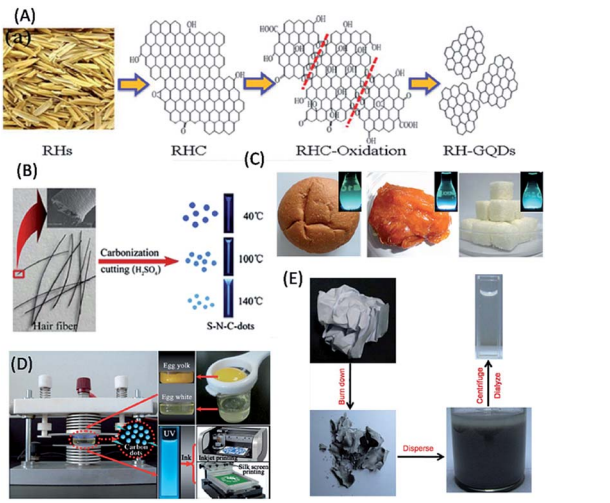

Fig. 6 Use of biomass and their wastes. (A) Rice husk, (B) human hair, (C) bread, jaggery and sugar cubes, (D) eggs and (C) paper ash as carbon sources for the fabrication of biomolecule-derived QDs. (A) has been adapted/reproduced from ref. 100 with permission from the American Chemical Society, (B) from ref. 109 with permission from Elsevier, (C) from ref. 113 with permission from John Wiley and Sons, (D) from ref. 114 with permission from Springer Nature, and (E) from ref. 121 with permission The Royal Society of Chemistry.

a QY of 3.8% and excitation-dependent tunable emission in the range of 400–600 nm and also demonstrated their usefulness in cellular imaging and analytical applications.[104] Sun and co-workers demonstrated that the hydrothermal treatment of grass resulted in the formation of carbon-based biodots with a QY in the range of 2.5% to 6.2% based on the temperature and demonstrated their use in the label-free sensing of Cu^{2+} ions.[105] Ogale and co-workers showed the use of dead neem leaves, as a natural and waste source of carbon, for the large scale synthesis of green fluorescent G-QDs (with a QY of 1%). Subsequent passivation with amine resulted in a shift in their to blue with an enhancement in QY from 1% to 2%, and finally the amine-passivated G-QDs were used for the efficient and selective sensing of Ag^{+} ions.[106] The electro-oxidation of wood charcoal was demonstrated as a cheap and green method for the synthesis of highly blue luminescent G-QDs, which efficacy in the sensing of glucose and hydrogen peroxide.[107]

According to earlier reports, animals and their derivatives (silkworm chrysalis, human hair, cow manure, bird feathers, human urine *etc.*) were used as carbon raw material sources in the synthesis of carbon-based QDs.[108–112] For example, (i) Wang and co-workers reported the fabrication of highly blue luminescent N-doped C-QDs, (with a QY of 46%) from silkworm chrysalis *via* microwave-assisted synthesis, which were used as a cellular imaging agent.[108] (ii) Sun *et al.* reported the formation of blue luminescent (N, S) co-doped C-QDs with a QY of 11.1% and excitation wavelength-dependent tunable luminescence properties from the thermal decomposition of human hair fibers, and demonstrated their use as a bioimaging agent (Fig. 6B).[109] (iii) Cow manure was used as a carbon source to synthesize blue fluorescent low-toxicity C-QDs with a QY of 65% and the capability to selectively stain nucleoli in breast cancer cell lineages.[110] (iv) Liu *et al.* demonstrated the use of bird feathers to fabricate blue fluorescent, water-soluble, heteroatom doped C-QDs *via* microwave-hydrothermal treatment, with a QY of 17.1% QY, excitation-tunable emission and capability to sense ferric ions.[111] (v) Baker and co-workers demonstrated that human urine-derived C-QDs (otherwise known as pee dots), with a maximum QY of 14% and blue color emission, could be synthesized *via* the carbonization of human urine. The biocompatible pee dots exhibited applicability in the multiplexed fluorescence imaging of mice embryonic fibroblast cells and in the detection of heavy metal ions.[112]

Foods (including bakery products and beverages) and their wastes are an important class of renewable carbon sources for the synthesis of carbon-based QDs.[113–119] Chattopadhyay and co-workers demonstrated the use of various food products (such as bread, corn flakes, biscuits, jaggery and sugar caramel) as carbon sources for the microwave-assisted synthesis of water-soluble nontoxic C-QDs, with excitation-tunable luminescence properties and QYs in the range of 0.63–1.2% (Fig. 6C).[113] Bright blue fluorescent C-QDs were obtained *via* plasma-induced synthesis using eggs (both their yolk and white parts) as the starting material, (with QY in the range of 6–8%), which were used as luminous inks for multicolor patterns using inkjet and silk-screen printing, by Wang *et al.* (Fig. 6D).[114] Mahesh *et al.* demonstrated the use of honey as a precursor for the carbonization-based fabrication of G-QDs with excitation-tunable luminescence and QY of 3.6%, which were used as a stable security ink and for the generation of white light emission.[115] Notably, overcooked barbeque meat was also used as a raw material for the synthesis of green luminescent C-QDs with excitation-dependent luminescence and QY in the range of 1–2%, which showed photocatalytic activity.[116] Further, C-QDs with a QY of 7.39% and excitation-dependent fluorescent characteristics were synthesized using beer as a starting material, which were eventually used for cellular imaging of breast cancerous cells and drug delivery.[117] Likewise, milk-derived C-QDs (*via* hydrothermal treatment of milk) with a QY of 9.6% and multicolor emissive properties were also reported.[118] In addition, hydrochar, a waste of food products, was used as a carbon precursor for the synthesis of multicolor (blue, green, yellow and red) C-QDs, with QYs in the range of 6–28%, which were used as a fluorescence probe for the detection of Fe^{3+} ions.[119]

In this regard, industrial waste products (lignin and paper ash) have also been used for the fabrication of scalable, nontoxic, highly luminescent biodots.[120,121] For example, Ding *et al.* showed that lignin, which is a natural source of aromatics and pulping industrial waste, could be used as a low-cost, green and sustainable raw material for the hydrothermal synthesis of blue luminescent G-QDs with a QY of 21% and excitation-dependent fluorescence behaviour, which showed potential in bioimaging applications.[120] Similarly, Wei *et al.* reported the formation of blue luminescent C-QDs, (with a QY of 9.3% and multicolour emissive behaviour depending on excitation wavelength) using paper ash as a carbon source, and subsequently demonstrated their use as a bio-labelling agent (Fig. 6E).[121]

The details of the remarkable optical properties (such as absorption, excitation, emission, and luminescence colour under UV light and QYs) and the synthetic methods of the reported biomolecule-derived QDs are presented in Table 1. This will be helpful for the fabrication of sustainable optoelectronic devices, based on the use of scalable, renewable and cost effective biomolecules.

3. Synthetic methods for biomolecule-derived QDs

3.1. Hydrothermal/solvothermal

Hydrothermal or solvothermal carbonization, which is based on heating precursor materials at a high temperature in a sealed container, is a low-cost, eco-friendly, and green route for the synthesis of C-QDs and G-QDs from various biomolecules.[1–30] For example, highly luminescent C-QDs and G-QDs have been synthesized through hydrothermal/solvothermal carbonization from numerous precursors, including plant extracts (such as orange juice,[31] pineapple peels,[39] cabbage,[46] and curcumin[49]), amino acids and proteins (such as histidine,[71] glutamic acid,[78] BSA,[81,84,85] and β-lactoglobulin[87]), nucleic acids, fungi and bacteria (such as DNA,[92] mushroom fungus,[96] and *L. plantarum*[99]) and biomass and their waste (such as rice husks,[100] dead neem leaves,[106] milk[118] and lignin[120]).

Table 1 Summary of the use of different biomolecules for the synthesis of biomolecule-derived QDs (C-QDs and G-QDs), synthetic methods and their optical properties (absorbance, excitation, emission, luminescence color and quantum yield)[a]

				Optical Features					
Carbon source		Synthetic method	Type of QDs	λ_{abs} (nm)	λ_{ex} (nm)	λ_{em} (nm)	Luminescence colour (under UV light)	QYs (%)	Ref.
Plant extracts	Orange juice	Hydrothermal	C-QDs	288	360–450	441–510	Green	26	31
	Banana juice	Simple heating	C-QDs	283	360	460	Green	8.95	32
	Apple juice	Hydrothermal	C-QDs	250, 300	368	475	Blue	4.27	33
	Papaya juice	Hydrothermal	C-QDs	250–350	383	461	Blue	7.0	34
	Pear juice	Autoclave	WAC-QDs	254	360	453	Blue-green	0.73	35
			AC-QDs	NOAP*	400	509	Blue-green-yellow-orange	3.82	
	Grape seeds	Microwave	G-QDs	220, 290	250	320	—	31.79	36
	Lychee seeds	Pyrolysis	C-QDs	NOAP*	365	440	Blue	10.6	37
	Watermelon peels	Pyrolysis	C-QDs	NOAP*	310–450	490–580	Blue	7.1	38
	Pineapple peels	Hydrothermal	C-QDs	—	—	—	Blue	42	39
	Orange peels	Hydrothermal	C-QDs	268	340	431	Blue	36	40
	Pomelo peels	Hydrothermal	C-QDs	280	365	444	Blue	6.9	41
	Plane	Pyrolysis	C-QDs	NOAP*	370	429	Blue	16.4	42
	Lotus					424		15.3	
	Pine leaves					427		11.8	
	Tea leaves	Simple heating	C-QDs	—	380–500	—	Blue	—	43
	Lotus roots	Microwave	C-QDs	280	360	435	Blue	19	44
	Rose flowers	Oven based baking	C-QDs	390	390	435	Blue	13.45	45
	Cabbages	Hydrothermal	C-QDs	276, 320	345	432	Blue	16.5	46
	Sweet potato	Hydrothermal	C-QDs	266	360	442	Blue	8.64	47
	Tomato	Microwave	C-QDs	298	340	420	Blue	1.77	48
	Curcumin	Hydrothermal	C-QDs	265, 345	280	—	Blue	8.607	49
	Spinach, peas, pepper, guava	Autoclave	C-QDs	270, 320	400	440	Blue	—	50
Simple sugars and polysaccharides	Glucose	Acid treatment	C-QDs	NOAP*	360	440	Blue	13	51
	Glucose	Microwave	C-QDs	280	330	425	Blue	6.3	52
	Glucose	Microwave	G-QDs	228, 282	375	473	—	7–11	53
	Glucose	Autoclave	C-QDs	276, 300	336	437	Blue	30	54
	Glucose	Heating	C-QDs	275, 336	403	502	Green	9.6	55
	Maltose + fructose	Base + dialysis	C-QDs	210, 270	400	500	Green	2.2	58
	Sucrose	Simple heating	C-QDs	250–300	375	590	Orange-red	15	59
	Glucosamine	Microwave	C-QDs	270	340	440	Blue	18	60
	Glycerol	Microwave	C-QDs	290	340–480	450–550	Blue to green	12	61
	Xylitol	Microwave	C-QDs	286	360	446	Blue	7	62
	Chitin	Autoclave	C-QDs	282	300	440	Blue	—	63
	Chitosan	Microwave	C-QDs	—	350, 400	397, 460	Blue	—	64
	Chitosan	Microwave	C-QDs	243	380	—	Green	—	65
	Alginic acid			243	370				
	Starch			242	370				

Table 1 (*Contd.*)

Carbon source		Synthetic method	Type of QDs	Optical Features					
				λ_{abs} (nm)	λ_{ex} (nm)	λ_{em} (nm)	Luminescence colour (under UV light)	QYs (%)	Ref.
	Cellulose	Hydrothermal	C-QDs	272, 315	330	410	Blue-green	21.7	66
	Cyclodextrin	Hydrothermal	C-QDs	—	420	510	Green	13.5	67
	β-Cyclodextrin	Heating	C-QDs	280, 320	390	510	Green	30	68
	Hyaluronic acid-glycine	Autoclave	C-QDs	300–550	360	470	Blue	—	69
Amino acids and proteins	Histidine	Microwave	C-QDs	299	360	440	Blue	44.9	70
	Histidine	Hydrothermal	C(60)-QDs	294	360	439	Blue	8.9	71
	20 different natural α-amino acids (ser and thr)	Autoclave	C-QDs (AA dots)	240, 270	360	450	Blue	30.44	72
	L-Ser and L-cys	Autoclave	C-QDs	NOAP*	540	610	—	—	73
	L-Spartic acid	Heating	C-QDs	277, 332	380, 460	465, 550	Blue	7.5	74
	Cysteine	Heating	C-QDs	270	350	444	—	38	75
	Lysine	Heating	C-QDs	—	350	400–500	Blue	—	76
	Isoleucine	Hydrothermal	C-QDs	242, 343	370	415	Blue	—	77
	Glutamic acid	Hydrothermal	C-QDs	—	360	—	Blue	30.7	78
	Glutamic acid	Heating	G-QDs	238, 335	360	440	Blue	54.5	79
	Glycine	Heating	G-QDs	240, 330	380	450	Blue	16.2	80
	BSA	Hydrothermal	C-QDs	276	360	448	Blue	11	81
	BSA	Hydrothermal	C-QDs	—	380	450	Blue	34.8	82
	Denatured BSA	Microwave	C-QDs	236, 283	360	400	Blue	14	83
	BSA	Hydrothermal	C-QDs	360	390	465	Blue	44	84
	BSA	Hydrothermal	C-QDs	275	320	407	Blue	17.1	85
	BSA	Autoclave	C-QDs	230, 280	360	440	Blue	7	86
	β-Lactoglobulin	Hydrothermal	C-QDs (EDA)	280, 317	375	458	Blue	56	87
	Hemoglobin	Muffle furnace	C-QDs	—	230	380	Blue	3.9	88
	Gelatin	Hydrothermal	C-QDs	250–290	350	430	Blue	31.6	89
Nucleic acids, fungus and bacteria	DNA	Autoclave	C-QDs	260, 300–400	370	465	Blue	3.65	91
	DNA	Hydrothermal	C-QDs	280	290	420	Blue	1.1	92
	DNA	Autoclave	C-QDs	270, 280–350	275	Around 400, 460	Blue	—	93
	Bacterial genomic DNA	Hydrothermal	C-QDs	NOAP*	366	445	Blue	—	94
	Mushroom fungus	Thermal treatment	C-QDs	292	360	456	Blue	25	95
	Mushroom fungus	Hydrothermal	C-QDs	285	370	455	Blue	15.3	96
	S. aureus, *E. coli* bacteria	Hydrothermal	C-QDs	256, 328	320	400	Bluegreen	7.0, 8.1	97
	Cyanobacteria	Ultrasound irradiation	C-QDs	—	350–610	300–500	—	—	98
	L. plantarum	Hydrothermal	C-QDs	NOAP*	380	450	Blue	10.3	99
Biomass and their waste	Rice husk	Hydrothermal	G-QDs	—	310–340	360–440	Blue	8.1	100
	Sugar cane molasses	Thermal treatment	C-QDs	260, 320	305	390	Blue	5.8	101
	Bagasse	Hydrothermal	C-QDs	275	370	475	Blue	12.3	102
	Chia seeds	Thermal treatment	C-QDs	265, 280, 325, 350	—	—	Blue, green, yellow	10	103
	Coffee grounds	Simple heating	C-QDs	—	365	440	Blue	3.8	104
	Grass	Hydrothermal	C-QDs	280	360	443	Blue	6.2	105
	Dead neem leaves	Hydrothermal	G-QDs	300	350	—	Green	1	106

Table 1 (*Contd.*)

Carbon source	Synthetic method	Type of QDs	Optical Features					
			λ_{abs} (nm)	λ_{ex} (nm)	λ_{em} (nm)	Luminescence colour (under UV light)	QYs (%)	Ref.
		Am G-QDs				Blue	2	
Wood charcoal	Electro oxidation	G-QDs	220, 290	325	450	Blue	—	107
Silkworm chrysalis	Microwave	C-QDs	220, 276, 317	350	420	Blue	46	108
Human hairs	Thermal decomposition	$(C\text{-}QDs)_{40}$	323	330	383	Blue	11.1	109
Cow manure	Oven heating	C-QDs	—	—	—	Blue	65	110
Bird's feathers (Goose)	Microwave-hydrothermal	C-QDs	270	340	410	Blue	17.1	111
Human's urine	Heating, carbonization	UPD	330, 390	325	392	Blue	5.3	112
		CPD	330, 385	350	427		4.3	
		APD	325, 400	425	500		2.7	
Jaggery, sugar caramel and bread	Microwave	C-QDs	240–400	375	—	Blue	0.55, 0.63 and 1.2	113
Egg	Plasma induced	$(C\text{-}QDs)_{pew}$	275	360	420	Blue	6	114
		$(C\text{-}QDs)_{pey}$					8	
Honey	Carbonization	G-QDs	267, 340	340	435	Green	3.6	115
BBQ meat	Thermal annealing	C-QDs	NOAP*	440	520	Green	40	116
Beer	Column separation	C-QDs	270	340	420	Blue	7.39	117
Milk	Hydrothermal	C-QDs	274	379	448	Blue	9.6	118
Hydrochar	Hydrothermal	C-QDs	—	370–460	Multicolour	Blue	28	119
			—	400–470	emission	Green	18	
			420	450–570		Yellow	10	
			440	450–570		Red	6	
Lignin	Hydrothermal	G-QDs	290, 350	310	410	Blue	21	120
Paper ash	Sonication, dialysis	C-QDs	263	365	446	Blue	9.3	121

[a] NOAP* stands for no obvious absorption peak. It should be mentioned here that for all the biomolecule-derived QDs, their excitation and emission are selected based on the maximum intensity, despite their excitation tunable emission properties.

3.2. Microwave irradiation

Microwave irradiation is an efficient, eco-friendly and rapid method for the fabrication of biomolecule-derived QDs. Typically, the biomolecule (followed by dissolving in a solvent) is heated in a microwave chamber. For example, C-QDs and G-QDs have been synthesized *via* microwave irradiation from many precursors including plant extracts (such as grape seeds,[36] lotus roots,[44] tomato,[48] *etc.*), simple sugars and polysaccharides (glucose,[52,53] glucosamine,[60] glycerol,[61] xylitol,[62] and chitosan[64]), amino acids and proteins (such as histidine,[70] denatured BSA,[83] BSA,[81,84,85] and β-lactoglobulin[87]), and biomass and their waste (such as silkworm chrysalis,[108] jaggery, sugar caramel and bread[113]).

3.3. Pyrolysis

In the pyrolysis method, initially, decomposition of the biomolecules above their melting points occurs followed by condensation and nucleation, which lead to the formation of C-QDs and G-QDs.[1–30] Earlier reports showed that pyrolysis has been used as a synthetic strategy for the fabrication of biomolecule-derived QDs. For example, using pyrolysis, C-QDs and G-QDs have been fabricated from many biomolecules such as lychee seeds,[37] watermelon peels,[38] and plane, lotus, and pine leaves.[42]

3.4. Simple heating

Besides heating in sophisticated instruments, simple thermal treatment has also been used to synthesize high-quality biodots.[1–30] Earlier reports showed that C-QDs and G-QDs could be fabricated *via* simple heating using many biomolecules, such as banana juice,[32] tea leaves,[43] glucose,[55] sucrose,[59] β-cyclodextrin,[68] L-aspartic acid,[74] cysteine,[75] lysine,[76] chia seeds,[103] coffee grounds,[104] and cow manure.[110]

3.5. Autoclaving and plasma treatment

In a similar manner, biomolecule-derived C-QDs and G-QDs have also been fabricated *via* autoclaving and plasma treatment.[1–30] For example, pear juice,[35] spinach, peas, pepper, guava,[50] chitin,[63] L-ser and L-cys,[73] BSA,[86] and DNA,[91,93] have been used to synthesize biodots *via* pyrolysis, while plasma treatment of eggs resulted in the formation of C-QDs.[114]

3.6. Sonication

Alternating low- and high-pressure waves in liquid with strong hydrodynamic shear forces make ultrasound methods important synthetic methods for the construction of biomolecule-derived QDs.[1–30] This is a simple, low-cost and environment friendly route for the synthesis of C-QDs and G-QDs. For example, the ultrasound method has been used to synthesize biomolecule-derived QDs from many precursors ranging from cyanobacteria[98] to paper ash (a biomass waste).[121]

3.7. Chemical treatment

Despite their harshness, the treatment of biomolecules with chemical agents such as acids and bases for the synthesis of biodots (C-QDs and G-QDs) has also been reported.[1–30] For example, the treatment of glucose with acid[51] and a mixture of maltose and fructose with base[58] resulted in the formation of biomolecule-derived C-QDs. Similarly, electrochemical oxidation has also been used to synthesize biodots from wood charcoal.[107]

4. Origin of absorption and luminescence of biomolecule-derived QDs

The fabrication of optoelectronic devices using biomolecule-derived QDs solely depends on their remarkable optical features such as high QY, emission colour, excitation-tunable emission, photostability, and separation of charge carriers. This circumvents problems related to the fabrication of biomolecule-based nano optoelectronic devices. However, very little attention has been paid to elucidating the clear and plausible mechanism of the origin of the luminescence of biomolecule-based QDs (especially, C-QDs and G-QDs). On the other hand, the aforementioned optical properties (such as absorbance and luminescence) of biomolecule-derived QDs (C-QDs and G-QDs), including their amorphous and crystalline natures, are found to be quite similar to the optical properties exhibited by C-QDs and G-QDs synthesized using man-made carbon precursors.

It is clear from Table 1 that all the biomolecule-derived QDs absorb mostly in the UV region in the range of 200–400 nm, with the occasional minimum absorption in the blue window. This is correlated with the two primary electronic transitions, π–π^* and n–π^*, of the C=C and C=O/heteroatom bonds.[1–3] This indicates that irrespective of the size of the biomolecules used during the synthesis of C-QDs and G-QDs, their small surface functional groups are responsible for their optical absorption. This also directs the scope of possibility of surface functionalization for better and advanced properties of C-QDs and G-QDs.

Several research groups have demonstrated their speculation regarding the origin of luminescence, high QY, photostability and excitation tunable luminescence properties of C-QDs and G-QDs based on the use of different carbon sources and reaction conditions. For example, Peukert and co-workers showed that the structure of the species present on the surface of C-QDs efficiently controls their properties, mainly quantum yield and photostability, and thus demonstrated that the surface structure of C-QDs plays an important role in their remarkable optical features.[122,123] Notably, Guldi and co-workers revealed the relation between surface defect states and optical features of C-QDs based on the observation of spectroscopic and electrochemical properties (especially redox-dependent optical behaviour) and showed the presence of two different emitting states (mono and bimodal), although the exact interpretation of the electronic states is rather difficult.[124–126] Thus, the luminescence properties of C-QDs may be mostly due to the surface-confined recombination of electron and holes, as depicted from earlier observations, while the size-dependent luminescence also originates from the quantum confinement effect of C-QDs

(although scarcely reported).[124–126] Importantly, according to earlier reports based on experimental observations and theoretical calculations, the origin of the luminescence of G-QDs depends on the quantum confinement effect of the conjugated π-electrons in the sp^2 carbon domain.[1–3] Thus, control over the π-electron conjugation with regard to the alteration in size, shape, elemental doping (N, S), surface defects and functionalization, is essential for anticipated optoelectronic applications. However, the understanding of the luminescence behaviour of C-QDs and G-QDs is still uncertain and not precisely defined. Thus far, the speculations of surface functional groups (or charges), oxidation activity of the surface, elemental doping, and conjugated sp^2 domain effect depending on reaction conditions in addition to the quantum size effect are the basic concepts behind the origin of C-QDs and G-QDs, which have been demonstrated since their discovery.[127–131] As is clear from the resemblance in the luminescence properties of C-QDs and G-QDs derived from biomolecules, which have similar optical features to man-made C-QDs, the aforementioned prime explanations such as surface structures (surface-confined charge carriers and defects) and conjugated sp^2-domains (quantum size effects) may be extended towards the fluorescence origin, tunable luminescence, high QY, and photostability of biomolecule-derived QDs.

5. Optoelectronic applications of biomolecule-derived QDs

5.1. Advantages of biomolecule-derived QDs for sustainable optoelectronics

As discussed above, biomolecule-derived QDs have been demonstrated to have application in biodiagnostics; however, their optoelectronics applications are yet to be fully explored (Fig. 7). The fabrication of advanced, renewable and low-cost optoelectronic devices, such as LEDs, display systems, solar cells, and photodetectors, are important and in demand towards finding alternatives to fossil fuel-based energy sources, and thus to mitigate the global energy crisis.[2,29,132–166] This is completely based on the properties of materials with regard to their abundance, low-cost, scalability and extraordinary optical properties (such as QY, lifetime, and photo-bleaching resistivity).[2,29,132–166] Metal-based QDs and other fluorophores (such as organic dyes and polymers) have shown applicability in this regard; however, their real-life application is restricted due to problems related to their toxicity, low optical performance (such as photodegradation and low quantum yield) and scalability for real-life device fabrication.[2,29,132–166] On the other hand, carbon-based nanoscale materials (C-QDs and G-QDs) have been emerged as promising candidates for the real-life application of optoelectronic devices.[2,29,132–166] To date, several research groups have demonstrated the use of different C-QDs and G-QDs as a optoelectronic materials for application in the fabrication of LEDs, displays, solar cells and photodetectors.[2,29,132–166] However, the use of biomolecule-derived QDs (including C-QDs and G-QDs) in the aforementioned uses of optoelectronics is yet to be fully explored. The additional advantages of scalability (in terms of product yields, although scarcely reported to date), renewability and cost-effectiveness, in addition to the similar advantages (such as eco-friendliness, low cytotoxicity, high QY, long emission lifetime, and photostability) of man-made C-QDs and G-QDs and traditional fluorophores (such as metal-based QDs, organic dyes and polymers), make biomolecule-derive C-QDs and G-QDs exceptional and promising alternatives for the fabrication of optoelectronic devices with enhanced performances.[2,29,132–166] Specifically, the use of man-made C-QDs and G-QDs and other fluorophores (such as metal-based QDs, organic dyes and polymers) has been extensively demonstrated in optoelectronics; whereas, biomolecule-derived QDs, which

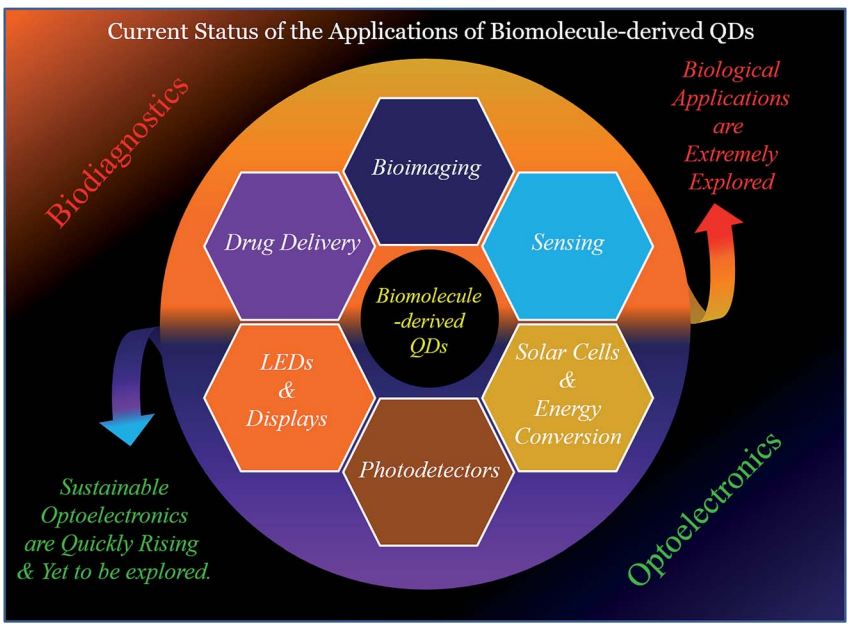

Fig. 7 Schematic illustration of the different uses, which are mainly biodiagnostics and optoelectronic purposes, of biomolecule-derived QDs.

have similar and/or enhanced physical properties with the additional advantages of scalability, cost-effectiveness and renewability (which are required for real-life practical utilization), have only recently started to gain attention for the advancement of optoelectronics.

Hence, this part of the review discussed the optoelectronic uses of man-made C-QDs and G-QDs thus far (briefly), which are required for the future applications of biomolecule-derived C-QDs and G-QDs in optoelectronics, which have not yet been similarly used. Since the optoelectronic applications of biomolecule-derived QDs are not yet fully explored, a brief discussion on the optoelectronics uses of manmade C-QDs and G-QDs its important with regard to their future scope of applicability. Importantly, the other main part demonstrates the optoelectronic uses (such as in LEDs, especially, white light-emitting ones, display systems, solar cells, energy conversion processes and photodetectors) of biomolecule-derived C-QDs and G-QDs since their discovery. Essentially, the aforementioned advantages and limitations (including band gap, crystallinity and higher temperature sustainability issues) and their possible solutions of optoelectronic devices based on biomolecule-derived QDs will be discussed in the next section as challenges and opportunities. The use of biomolecule-derived QDs for optoelectronic purposes is subdivided based on their use in different optoelectronic applications, which are discussed as follows.

5.2. Light-emitting devices (white LEDs)

The prime focus of solid-state lighting research, especially the fabrication of LEDs and displays, relies on the sustainability and environmental friendliness of luminescent nanomaterials, with extraordinary optical features in terms of QY, lifetime, photostability and other light-emitting parameters (such as colour chromaticity, colour rendering index (CRI) and correlated colour temperature (CCT)).[2,132–146] The traditional approaches for the fabrication of LEDs are mostly based on the use of environmentally unfriendly materials and complicated fabrication procedures, which restrict their real-life application in indoor and outdoor lighting.[2,132–146] This brings a new paradigm towards the fabrication of LEDs and displays using natural and biological sources, which are biocompatible in nature and have anticipated optical properties. Importantly, the combined tunable emission properties and biocompatibility of biomolecule-derived QDs make them a unique choice for the fabrication of LEDs and displays with different colour outputs, and thus towards the progress of solid-state lighting research.[2,136–146] It should be mentioned that control over the chromaticity, CRI and CCT defines the efficiency of a material for the construction of LEDs, and thus tuning of these properties is important.

The abovementioned properties of biomolecule-derived QDs definitely fit the requirements for the fabrication of biofriendly LEDs. Hence, it is noteworthy to focus on the sustainable optoelectronic applications of the aforementioned biomolecule-derived QDs, with tunable optical features and biocompatibility.

On the other hand, the fabrication of biofriendly, low cost and single white LEDs (WLEDs) stands out as one of the main and recent interests for sustainable optoelectronics to solve the problems associated with the global energy consumption.[2,136–146] However, the problems associated with the self-absorption, nonradiative energy transfer, energy consumption and undesirable changes in chromaticity coordinates restrict the real-life application potential of multicomponent-based white LEDs (such as coating of yellow phosphors on blue LEDs or mixing of three primary colour emitting nanostructures).[2,136–146] This has created a platform for the construction of single-component white LEDs with properties close to day-time bright light for the advancement of sustainable and environment-friendly optoelectronics. In this regards, different nanostructures (mostly semiconductor QDs) have been used to fabricate WLEDs; however, there are very few reports on the development of sustainable optoelectronic devices using biomolecule-derived QDs.[2,136–146] It should be mentioned that the perfect WLE material exhibits colour chromaticity coordinates of (0.33, 0.33), CRI at and above 80 and CCT in the range of 600–8000 K.[2,136–146] Hence, a brief summary of the light-emitting uses of man-made material-based C-QDs and G-QDs, in addition to that of biomolecule-derived QDs are summarized in the following section.

Interestingly, the excitation tunable multicolour emission properties of C-QDs and G-QDs have also been demonstrated for their use in fabricating different colour LEDs through the whole visible window. Specifically, LEDs ranging from blue-green-yellow-orange-red have been fabricated using C-QDs and G-QDs irrespective of the use of man-made and biomolecule resources.[2,136–146] Besides this, and as discussed above, the construction of WLED devices/materials is challenging. In this regard, C-QDs and G-QDs derived from man-made materials and natural resources have been demonstrated for the fabrication of WLE materials or devices. For example, (i) a cascade energy transfer-based WLED material with a QY of 19% and colour chromaticity coordinates of (0.33, 0.36) was fabricated using C-QDs.[136] (ii) Coating of yellow fluorescent C-QDs derived from *N*-acetylcysteine and combination of citric acid and urea on blue LED chips resulted in the formation of WLEDs.[137,138] (iii) The ratiometric combination of silane-functionalized green and red emitting C-QDs, followed by their coating on blue LEDs, resulted in the emission of white light with colour chromaticity coordinates close to (0.33, 0.33).[139] (iv) Acidic treatment followed by reduction to graphene sheets led to the formation of WLE G-QDs with chromaticity coordinates of (0.30, 0.36).[140] (vi) Generation of white light emission was also observed after the functionalization of the edge of GQDs prepared from graphite.[141]

Regarding the discussion of WLE devices/materials, based on the use of biomolecule-derived QDs, there are scarce reports in the literature. For example, (i) glucose-derived C-QDs, followed by coating on a blue LED were used as a single light converter for white LEDs with chromaticity coordinates of (0.28, 0.37) and CCT of 5584 K.[142] (ii) Honey-derived green luminescent G-QDs in combination with orange-red emissive rhodamine-B dye led to the formation of a WLE system with

chromaticity coordinates of (0.287, 0.310).[143] (iii) Hydrothermally synthesized glucose-derived C-QDs, followed by freeze drying showed white light emission.[144] (iv) Combined with red light-emitting chlorophyll and blue light-emitting quinine sulphate, green-emitting G-QDs (with a QY of 41.2%) derived from neem and fenugreek leaves were used to generate white light emission (Fig. 8A).[145] (v) The fabrication of WLE devices based on the formation self-assembled super-small C-QDs derived from heating- and pH-based synthesis using L-serine and L-tryptophan as carbon sources was reported by Lu *et al.* (Fig. 8B).[146] However, the use of various types of biomolecule-derived QDs towards the fabrication of WLE materials, especially single-component ones with better chromaticity, CRI and CCT parameters, is yet to be explored. The above discussion demonstrates that there is still vast scope to develop single WLE materials based on the use of biomolecule-derived QDs and manmade material-based QDs, which will be discussed in the Challenges and opportunities section of this review.

5.3. Solar cells and energy conversion

As an alternative of fossil fuel-based energy sources, numerous nanoscale materials have been used in the fabrication of highly efficient, green, low cost and scalable photovoltaic devices, especially solar cells (SCs).[2,29,147–156] To date, most of the SCs (such as organic SCs, silicon based SCs, and dye/QD-sensitized SCs (DSSCs/QDSSCs)) are based on the use of toxic nanomaterials, with a lack of scalability, renewability and maximum power conversion efficiency.[2,29,147–156] In this regard, the eco-friendly, inexpensive biomolecule-based C-QDs and G-QDs, with the scope of scalability and renewability and alluring optical features, have started to gain interest due to their different photovoltaic activities, such as sensitizers and photo-absorption agents (due to their absorption tail in the visible zone), charge carrier sources, and bridges and funnels (due to their large π-electron network (sp^2 core) and electron donating and accepting capability).[2,29,147–156] Importantly, the use of man-made material-based C-QDs and G-QDs has been displayed to have applicability in developing heterojunction solar cells devices (ZnO QDs/G-QDs and CDs/Si: with enhanced absorption and suppressed recombination and thus higher efficiency compared to their parent components), open circuit voltage increment in devices (depending on the quantum size effect of the G-QDs), solution-processed organic/metal oxide and dye-sensitized solar cells (such as combination of poly(3-hexylthiophene) (P3HT) and GQDs, and TiO_2 with G-QDs and C-QDs), *etc.*[2,147–151] However, we will describe these in detail since there are ample articles and reviews discussing this topic. As is clear from the similar properties of biomolecule-derived QDs with man-made carbon-based QDs, they are useful candidates for the same applications. Considering the use of biomolecule-derived C-QDs and G-QDs in photovoltaic devices, to date, there are only a few articles that report the use of natural product-derived QD based solar cells. For example, blue luminescent water-soluble bamboo-derived C-QDs (with a QY of 4.2%) were used as a cathode interfacial layer (Fig. 9A).[152] C-QDs in combination with ZnO increased the power conversion efficiency (PCE) of fullerene and non-fullerene organic photovoltaic devices (OPV) and the highest PCE of the OPV was 9.6% (with remarkable fill factor of 72.8%), as reported by Chen and co-workers. Importantly, Titirici and co-workers showed that the C-QDs derived from three different biomass sources (glucose, chitosan and chitin) could be used as a sensitizer in

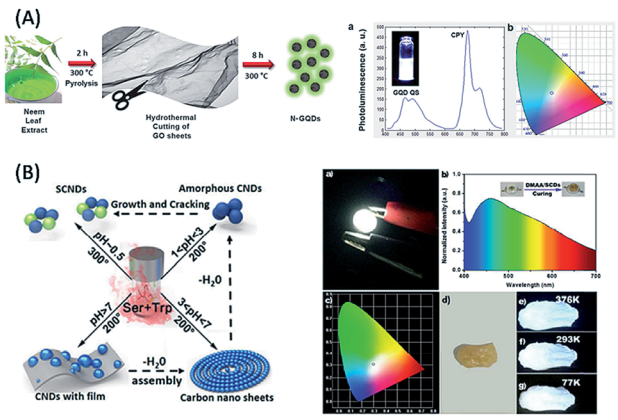

Fig. 8 Use of (A) neem leaf extract and (B) mixture of amino acids (Ser and Trp) for the synthesis of biomolecule-derived QDs and there by their use in white light generation and fabrication of WLE devices. (A) has been adapted/reproduced from ref. 145 with permission from the Centre National de la Recherche Scientifique (CNRS) and (B) from ref. 146 with permission from the American Chemical Society.

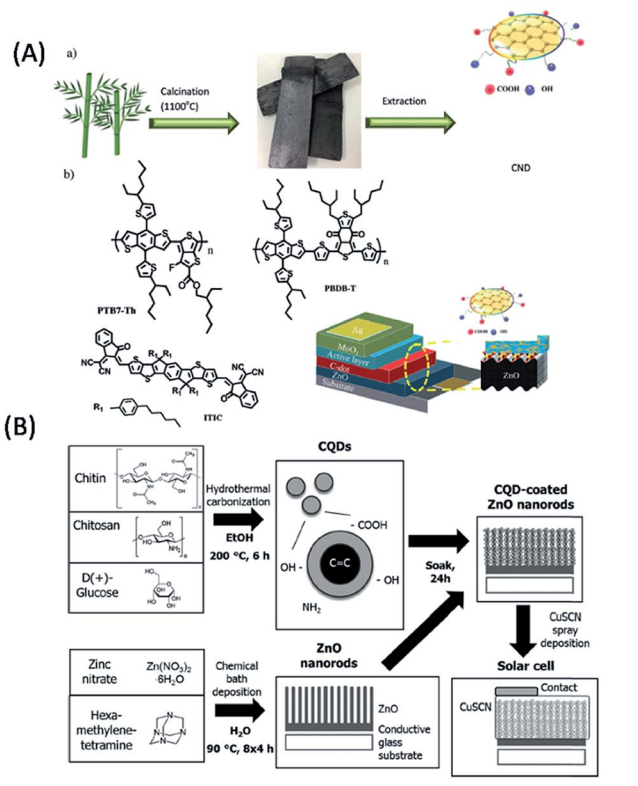

Fig. 9 Use of (A) bamboo- and (B) chitin-, chitosan- and glucose-derived QDs for the fabrication of solar cells. (A) has been adapted/reproduced from ref. 152 with permission from John Wiley and Sons and (B) from ref. 153 with permission from John Wiley and Sons.

a photovoltaic device with the architecture of FTO/ZnONanorods/CQDs/CuSCN/Au, and the highest efficiency of 0.077% was found for the layer based on the combination of chitosan and chitin-derived C-QDs (Fig. 9B).[153] Guo *et al.* showed that the hole transfer ability and small size of the C-QDs derived from the hydrothermal-based synthesis of bee pollen, citric acid, and glucose make them suitable for the fabrication of solar cells with highest efficiency of 0.11%.[154] Recently, Marinovic *et al.* reported the highest PCE of 0.36% for TiO_2-based solar cells sensitized by C-QDs derived from L-arginine followed by hydrothermal treatment, among the families of mono/polysaccharides (D-glucose, chitosan and chitin from lobster shells) and amino acids (L-arginine and L-cysteine).[155] Meng *et al.* demonstrated the use of C-QDs derived from the hydrothermal treatment of soybean powder for the fabrication of all-weather solar cells, which exhibited a dark power conversion efficiency as high as 7.97%.[156]

Besides their solar cell applications, the photocatalytic activities of C-QDs and G-QDs towards various energy conversion processes such as H_2 evolution (to alleviate fossil fuel scarcity and solve environmental problems) and CO_2 reduction/conversion (driven by environmental and economic issues), which are important with regard to the current demand of energy crisis, have also been demonstrated by several research groups.[7,157–163] Particularly, the use of biomolecule-derived QDs (C-QDs and G-QDs) will be focused on in the following section.[157–163] For example, (i) Reisner and co-workers demonstrated the use of C-QDs derived from L-aspartic acid as a photosensitizer to increase the catalytic activities of NiP-based catalysts and the charge transfer from C-QDs to NiP in the presence of a hole scavenger, which resulted in the production of 7950 μmol^{-1} h^{-1} of H_2 under visible light irradiation.[159] (ii) Interestingly, the modification of the g-C_3N_4 surface with L-ascorbic acid-derived C-QDs, in which electron transfer occurred from g-C_3N_4 to the C-QDs, resulted in H_2 production of 183.0 μmol^{-1} h^{-1} under visible light irradiation, as described by Ong *et al.*[160] (iii) Similarly, the nanocomposite synthesized using silver (Ag) nanoparticles (acted as a light harvester), g-C_3N_4 and glucose-derived C-QDs (acted as an electron donor to g-C_3N_4 and acceptor to Ag nanoparticles) resulted in the generation of 626.93 μmol g^{-1} h^{-1} of H_2 in the presence of a hole scavenger, according to the report of Qin *et al.* (Fig. 10A).[161] (iv) As reported by Li *et al.*, glucose-derived C-QDs in combination with Cu_2O were used as a photocatalyst for the conversion of CO_2 to methanol under visible light, with a yield of 55.7 μmol g^{-1} h^{-1} (Fig. 10B).[162] (v) Glucose-derived C-QDs combined with g-C_3N_4 sheets showed photocatalytic activity and resulted in the visible light conversion of CO_2 to CH_4 (29.23 μmol $g_{catalyst}^{-1}$) and CO (58.82 μmol $g_{catalyst}^{-1}$).[163] Nevertheless, C-QDs and G-QDs derived from different biomolecules have not been extensively used for solar cell applications and energy conversion processes. Therefore, there is vast scope and opportunities for biomolecule-based QDs towards the fabrication of low-cost, scalable and renewable solar cells/photocatalysts with high efficiencies, which will be discussed in detail in the Challenges and opportunities section.

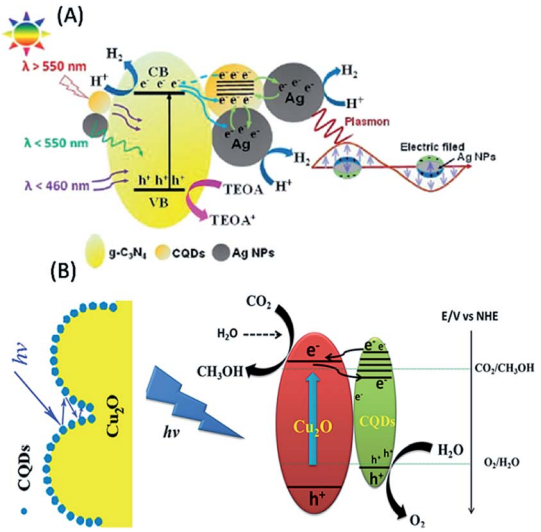

Fig. 10 Use of glucose-derived QDs for (A) the generation of H_2 gas and (B) conversion of CO_2 to methanol. (A) has been adapted/reproduced from ref. 161 with permission from John Wiley and Sons and (B) from ref. 162 with permission from Elsevier.

5.4. Photodetectors

Photodetectors with p–n or p–i–n junction diode structures or bipolar transistor structures are important optoelectronic devices for imaging, communication, automatic control, and biomedical sensing.[164–166] In this regard, metal semiconductors have been used in the construction of photodetectors; however, their use is limited mainly due to the costly and complicated device fabrication processes.[164–166] Hence, the development of simple and highly efficient photodetectors with the scope of scalability and renewability of their materials is extremely desirable and in demand. The separation of photo-generated carriers, which is the reverse process of luminescence recombination, is required for the fabrication of photodetectors.[164–166] Despite having excellent optical characteristics, good electrical conductivity is another prime concern for the materials used for the fabrication of photodetectors. C-QDs and G-QDs (irrespective of their synthesis from manmade materials or biomolecules) with deep UV photoluminescence and photo detection ability (due to their π–π*-based absorption mainly in the UV region) have been used in the fabrication of photodetectors.[164–166] Importantly, rather than using C-QDs and G-QDs directly in photodetectors, they have been combined with other materials for the better designing of device structure and band alignment, thus resulting in advanced photodetectors with higher performances. The use of non-biomolecule-based C-QDs and G-QDs as materials for the fabrication of photodetectors has also been reported. For example, G-QDs (synthesized based on the hydrothermal reduction of graphene oxide) combined with asymmetric electrodes of Au and Ag, were used to fabricate deep-UV photodetectors, which were capable of detecting deep UV light with a wavelength as short as 254 nm with a fast response speed (Fig. 11).[166] Similarly, graphite powder-derived G-QDs were also used to fabricate photodetectors with high-efficient photocurrent behaviour. The G-QDs-

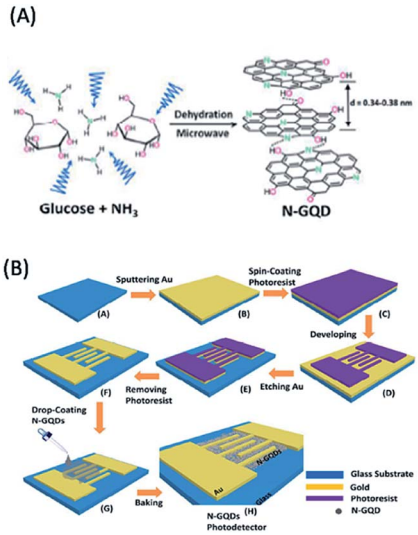

Fig. 11 Use of glucose-derived QDs for the fabrication of photodetectors. This figure has been adapted/reproduced from ref. 166 with permission from the American Chemical Society.

based photodetectors showed high detectivity (1011 cm Hz 1/2/W) and responsivity (0.2, 0.5 A/W) in a broad spectral range from UV to near infrared.[166] However, there are very few reports on the fabrication of photodetectors based on the use of biomolecule-derived C-QDs and G-QDs. For example, Tang *et al.* demonstrated the fabrication of nitrogen-doped G-QDs derived from glucose in the presence of aqueous ammonia, which exhibited deep UV-region absorbance properties (π–π^* transition) and broad emission spectra ranging from 300–1000 nm (due to the extensive delocalized π electrons of their layered structure).[166] Based on the coating of N-G-QDs on inter digital gold electrodes, broad band photodetectors having a responsivity of 325 V/W were fabricated and the observed negative photocurrent was explained with respect to the trapping sites of the self-passivated surface states of G-QDs. The above discussion shows that due to their poor crystallinity and conductivity, the use of C-QDs and G-QDs has not been explored extensively; however, this is also discussed in detail in the Challenges and opportunities section for the fabrication of biomolecule-derived QD-based photodetectors, followed by suggestions for solving the existing issues (Table 2).

Table 2 Summary of the optoelectronic uses of different biomolecule-derived QDs

Application	Type of QDs	Biomolecule used	Synthetic methods	Properties/role/utility	Ref.
LEDs	C-QDs	Glucose	Hydrothermal	Single light converter for white LEDs: with chromaticity coordinates of (0.28, 0.37) and CCT of 5584 K	142
	C-QDs	β-Carotene	Microwave	Donor (C-QDs)–acceptor (Rh-B)-based WLE system, having chromaticity coordinates of (0.33, 0.32)	143
	C-QDs	Glucose	Hydrothermal	Upon freeze drying, C-QDs showed white light emission	144
	G-QDs	Neem and fenugreek leaves	Hydrothermal	Multicomponent-based white light emission, with chromaticity coordinates of (0.31, 0.31) and CCT of 6849 K	145
	C-QDs	L-Serine and L-tryptophan	Heating and pH controlled	Self-assembled super small C-QDs: WLE devices with chromaticity coordinates of (0.29, 0.31)	146
Solar cells	C-QDs	Bamboo	Autoclave	Cathode interfacial layer; highest PCE of OPV is 9.6%	152
	C-QDs	Glucose, chitosan and chitin	Hydrothermal	Sensitizer; highest efficiency of 0.077%	153
	C-QDs	Bee pollen, glucose and citric acid	Hydrothermal	Hole transfer ability and small size, highest efficiency of 0.11%	154
	C-QDs	L-Arginine	Hydrothermal	Highest PCE of 0.36%	155
	C-QDs	Soybean powder	Hydrothermal	Dark power conversion efficiency as high as 7.97%	156
Energy conversion	C-QDs	L-Aspartic acid	Thermolysis	Photosensitizer; production of 7950 μmol^{-1} h^{-1} of H_2 under visible light irradiation	159
	C-QDs	L-Ascorbic acid	Hydrothermal	Electron acceptor; H_2 production of 183.0 μmol^{-1} h^{-1} under visible light irradiation	160
	C-QDs	Glucose	Alkali-auxiliary sonication	Electron donor and acceptor; generation of 626.93 μmol g^{-1} h^{-1} of H_2	161
	C-QDs	Glucose	Ultra-sonication	Photocatalyst; for the conversion of CO_2 to methanol with yield of 55.7 μmol g^{-1} h^{-1} under visible light	162
	C-QDs	Glucose	Alkali-assisted ultra-sonication	Photocatalyst; visible light conversion of CO_2 to CH_4 (29.23 μmol $g_{catalyst}^{-1}$) and CO (58.82 μmol $g_{catalyst}^{-1}$)	163
Photodetectors	N-doped G-QDs	Glucose	Microwave assisted hydrothermal	Deep UV-region absorbance properties and broad emission spectra ranging from 300–1000 nm; photodetectors: Having responsivity of 325 V/W	166

6. Challenges and opportunities

Despite the significant advancement in the area of optoelectronic devices using carbon-based QDs, the use of biomolecule-derived QDs (as listed above) for optoelectronic purposes is yet to be explored extensively. There are various issues that need to be solved for real-life optoelectronic applications. The prime concern is the mechanism behind the origin of their luminescence, which is still being debated. Thus, there is a lack of understanding regarding the convincing proof and acceptable explanation for the luminescence origin of biomolecule-derived C-QDs and G-QDs. In this direction, theoretical studies combined with experimental results are further needed. The dependence of optical properties on the size, shape, crystal nature, dopants and surface modification is still unclear and yet to be explored based on the combination of experiments and theory. Interestingly, the determination of the mechanism behind other properties such as photo-induced electron transfer and up-conversion luminescence of C-QDs and G-QDs is important and beneficial for their future versatile applications. In addition, the fabrication of high quality C-QDs and G-QDs completely depends on the synthetic and purification procedures. Hence, it will be highly desirable to fabricate pure C-QDs and G-QDs from biomolecules with enhanced optical features, and thus better uses. Apart from their fundamental issues, the optoelectronic application-specific issues of C-QDs and G-QDs derived from various biomolecules and their possible solutions are listed below.

6.1. LEDs issues

As tabulated above, most of the biomolecule-derived QDs exhibit blue to green luminescence, and thus high efficiency within the long wavelength emission window (in the range of yellow to red) is missing. Thus, highly efficient, longer emissive C-QDs and G-QDs derived from biomolecules are critical for the fabrication of white LEDs with excellent chromaticity, high CRI, and suitable CCT values. Although biomolecule-derived C-QDs and G-QDs possess excitation-tunable long wavelength emissions, their efficiency and low QY limit their application potential in the fabrication of white LEDs, with desired properties close to day-time bright light. Thus, the fabrication of highly efficient, longer wavelength emissive C-QDs and G-QDs derived from natural resources is much needed for the progress of white LEDs. Most importantly, the fabrication of a single component white light emitting material from C-QD or G-QD, which is the prime concern for solid-state lighting, is still a challenging task. Additionally, the higher temperature LED application of biomolecule-derived QDs is also challenging due to the degradation of biomolecules at higher temperature. This is expected to open up challenges for material chemists to come up with the idea of different elemental doping (which usually enhances the conjugation and thus generates narrower band gaps) and surface functionalization (which is needed for single-component WLE systems, self-assembly, structure design, and better stability, particularly at higher temperature with different luminescent molecules) to circumvent the aforementioned issues of biomolecule-derived QDs towards the fabrication of white LEDs, with desired properties and high performances. Additionally, energy transfer-based WLE systems using C-QDs and G-QDs derived from different biomolecule sources are still in a preliminary stage and yet to be fully explored. This will be based on the well-defined and atom-precise synthesis of QDs followed by manipulation of their surface defects either by doping or surface functionalization.

6.2. Solar cells and energy conversion issues

As is clear from the above discussion, most of the biomolecule-derived QDs absorb in the UV region (200–400 nm). However, the real-life applications of solar cells devices and energy conversion processes (besides photocatalysis) mostly depend on the absorption behaviour of materials in the visible and near infrared window for better efficiency, followed by maximizing the utilization of broad solar spectrum. Thus, the absorption of biomolecule-derived C-QDs and G-QDs in the UV region significantly restricts their application potential, for photocatalysis and consequently the construction of solar cells. Despite the various efforts of elucidating the donor and acceptor properties of C-QDs and G-QDs derived from fossil resources, a clear view of the photoinduced electron donor and acceptor properties of biomolecule-derived QDs will be noteworthy to fabricate highly efficient energy devices based on their donor–acceptor behavior with other materials and/or molecules. This will help to ease the process of fabrication of donor–acceptor-based solar cells. Additionally, the photostability of the oxygenated functional groups present on the surface of C-QDs and G-QDs is an essential issue during their use in energy conversion purposes. In this regard, the doping of various elements and surface functionalization are important factors to enhance the efficacy of biomolecule-derived QDs, followed by preservation of their photostability, in solar cells and energy conversion processes.

6.3. Photodetectors issues

The issues of the poor conductivity, low crystallinity and zero band gap nature of C-QDs and G-QDs derived from both synthetic and natural resources limit their applicability as photoactive materials, especially highly efficient photodetectors. Specifically, carbon-based photodetectors show lower photo-responsivity due to their zero band gap, low crystallinity and poor conductivity. Hence, there is a need to introduce new strategies for the synthesis, including surface functionalization, elemental doping and shrinking of their sizes, of C-QDs and G-QDs towards better quality materials (in terms of crystal nature, band gap and better conductivity) and highly efficient photodetectors.

Finally, the flexibility and wearability of biomolecule-derived QD-based optoelectronic devices (such as LEDs, solar cells and photodetectors) using dip-coating and roll to roll methods are important for their user-friendliness with better performances. This solely depends on the properties such as crystallinity, assembly and pinhole free films of the C-QDs and G-QDs derived from biomolecules. This highlights the need for the control of the surface of biomolecule-based C-QDs and G-QDs

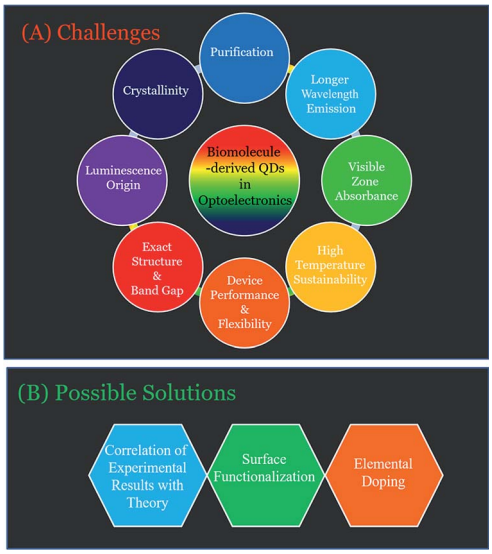

Fig. 12 Schematic illustration of the (A) challenges and (B) possible solutions of the biomolecule-derived QDs for their successful future sustainable optoelectronic uses.

through surface functionalization and doping. These challenges and opportunities are schematically summarized in Fig. 12.

7. Summary and future outlook

The present review documented the latest use of biomolecule-derived QDs (C-QDs and G-QDs) in various optoelectronic applications such as LEDs, solar cells, energy conversion, and photodetectors. In this review, we discussed the fabrication procedures, optical properties (such as absorption, excitation, emission maxima and colour, and quantum yield) and applications, especially for the sustainable development of optoelectronic devices (such as white LEDs, solar cells and photodetectors), of biomolecule-derived QDs (mainly C-QDs and G-QDs), which are eco-friendly, renewable and scalable. Importantly, based on the origin of the biomolecules (such as plant extracts, simple sugars and polysaccharides, amino acids and proteins, nucleic acids, bacteria, and biomass and their wastes), the C-QDs and G-QDs were classified with their optical features highlighted for their present and future optoelectronic applications. This review also showed how biomolecules are important to control the optical features of C-QDs and G-QDs, and thus for sustainable optoelectronic applications in demand and by choice.

The advantages of eco-friendliness, scalability, and renewability, in additional to their excellent optical features, make them more suitable candidates compared to traditional metal-based QDs and for application in LEDs, solar cells and photodetectors. The major issue of using biomolecules for any product of commercial importance is the yield of the products produced using the biomolecules. Notably, the good yields of the products (here QDs) derived from biomolecules (although scarcely reported to date) have caused them to become suitable choices for the fabrication and commercialization of sustainable optoelectronic devices.

Importantly, the Challenges and opportunity section discussed the specific issues regarding their application in LEDs, solar cells and energy conversion, and photodetectors, in addition to the fundamental issues of biomolecule-derived C-QDs and G-QDs, and also provided the possible solutions based on the use of simple chemical concepts. Briefly, improving the product yields, searching for new raw sources with high abundance, high optical performances, and purity, and determining the particular reasons and mechanisms behind their structure, band gap, luminescence and other physical and chemical properties (such as longer emissive wavelength and broad absorption) and device performance and flexibility are the some main challenges still to be explored. Accordingly, engineering biomolecule-derived QDs *via* surface functionalization and elemental doping, and improving the understanding by combined experimental results with theoretical calculations may have significant contribution towards sustainable optoelectronics applications.

Overall, the present review not only provides novel insights for the design of biomolecule-based QDs and their merits and disadvantages with respect to properties for specific and desired optoelectronic applications, but also brings a new avenue for scientists working in fields ranging from engineering to materials science towards future sustainable optoelectronics applications of eco-friendly QDs. Finally, the documented existing information on the synthesis, properties and optoelectronic applications of biomolecule-derived QDs with the existing challenges and future scope of this field will definitely inspire researchers to come up with innovative ideas, and thus progress in biomolecule-derived QD based sustainable optoelectronics.

Conflicts of interest

"There are no conflicts to declare".

Acknowledgements

The authors would like to thank Jain University, Bangalore, India for providing infrastructure to conduct this research work. S. Bhandari thanks the Department of Science & Technology (DST/INSPIRE/04/2017/001910; IFA17-CH287) Government of India for providing funding. D. Mondal thanks the SERB, India (EEQ/2017/000417) for the research grant.

Notes and references

1 X. Zhang, M. Jiang, N. Niu, Z. Chen, S. Li, S. Liu and J. Li, *ChemSusChem*, 2018, **11**, 11–24.
2 X. Li, M. Rui, J. Song, Z. Shen and H. Zeng, *Adv. Funct. Mater.*, 2015, **25**, 4929–4947.
3 S. Y. Lim, W. Shen and Z. Gao, *Chem. Soc. Rev.*, 2015, **44**, 362–381.
4 S. N. Baker and G. A. Baker, *Angew. Chem., Int. Ed.*, 2010, **49**, 6726–6744.

5 M. Titirici, R. J. White, N. Brun, V. L. Budarin, D. S. Su, F. Monte, J. H. Clark and M. J. MacLachlan, *Chem. Soc. Rev.*, 2015, **44**, 250–290.
6 R. Das, R. Bandyopadhyay and P. Pramanik, *Mater Today Chem.*, 2018, **8**, 96–109.
7 G. A. M. Hutton, B. C. M. Martindale and E. Reisner, *Chem. Soc. Rev.*, 2017, **46**, 6111–6123.
8 V. Sharma, P. Tiwari and S. M. Mobin, *J. Mater. Chem. B*, 2017, **5**, 8904–8924.
9 S. Zhou, H. Xu, W. Gan and Q. Yuan, *RSC Adv.*, 2016, **6**, 110775–110788.
10 X. T. Zheng, A. Ananthanarayanan, K. Q. Luo and P. Chen, *Small*, 2015, **11**, 1620–1636.
11 Y. Wang and A. Hu, *J. Mater. Chem. C*, 2014, **2**, 6921–6939.
12 J. Shen, Y. Zhu, X. Yang and C. Li, *Chem. Commun.*, 2012, **48**, 3686–3699.
13 R. Wang, K. Lu, Z. Tang and Y. Xu, *J. Mater. Chem. A*, 2017, **5**, 3717–3734.
14 F. R. Baptista, S. A. Belhout, S. Giordani and S. J. Quinn, *Chem. Soc. Rev.*, 2015, **44**, 4433–4453.
15 K. Hola, Y. Zhnag, Y. Wang, E. P. Giannelis, R. Zboril and A. L. Rogach, *Nano Today*, 2014, **9**, 590–603.
16 P. Zuo, X. Lu, Z. Sun, Y. Guo and H. He, *Microchim. Acta*, 2016, **183**, 519–542.
17 Y. Choi, Y. Choi, O. Kwon and B. Kim, *Chem.–Asian J.*, 2018, **13**, 586–598.
18 H. Ali, S. Ghosh and N. R. Jana, *MRS Adv.*, 2018, **3**, 779–788.
19 J. Zhou, H. Zhou, J. Tang, S. Deng, F. Yan, W. Li and M. Qu, *Microchim. Acta*, 2017, **184**, 343–368.
20 S. Bak, D. Kim and H. Lee, *Curr. Appl. Phys.*, 2016, **16**, 1192–1201.
21 S. Hill and M. C. Galan, *Beilstein J. Org. Chem.*, 2017, **13**, 675–693.
22 T. S. Atabaev, *Nanomaterials*, 2018, **8**, 342–352.
23 M. Han, S. Zhu, S. Lu, Y. Song, T. Feng, S. Tao, J. Liu and B. Yang, *Nanotoday*, 2018, **19**, 201–218.
24 J. Wang and J. Qiu, *J. Mater. Sci.*, 2016, **51**, 4728–4738.
25 M. K. Barman and A. Patra, *J. Photochem. Photobiol., C*, 2018, **37**, 1–22.
26 M. Tuerhong, X. Yang and Y. Xue-Bo, *Chin. J. Anal. Chem.*, 2017, **45**, 139–150.
27 K. Li, X. Zhao, G. Wei and Z. Su, *Curr. Med. Chem.*, 2018, **25**, 2876–2893.
28 M. Kaur, M. Kaur and V. K. Sharma, *Adv. Colloid Interface Sci.*, 2018, **259**, 44–64.
29 J. B. Essner and G. A. Baker, *Environ. Sci.: Nano*, 2017, **4**, 1216–1263.
30 A. Abbas, L. T. Mariana and A. N. Phan, *Carbon*, 2018, **140**, 77–99.
31 S. Sahu, B. Behera, T. K. Maiti and S. Mohapatra, *Chem. Commun.*, 2012, **48**, 8835–8837.
32 B. De and N. Karak, *RSC Adv.*, 2013, **3**, 8286–8290.
33 V. N. Mehta, S. Jha, H. Basu, R. K. Singhal and S. K. Kailasa, *Sens. Actuators, B*, 2015, **213**, 434–443.
34 B. S. B. Kasibabu, S. L. D'souza, S. Jha and S. K. Kailasa, *J. Fluoresc.*, 2015, **25**, 803–810.
35 J. Mondal and S. K. Srivastava, *ChemistrySelect*, 2018, **3**, 8444–8457.
36 M. K. Kumawat, M. Thakur, R. B. Gurung and R. Srivastava, *Sci. Rep.*, 2017, **7**, 15858.
37 M. Xue, M. Zou, J. Zhao, Z. Zhan and S. Zhao, *J. Mater. Chem. B*, 2015, **3**, 6783–6789.
38 J. Zhou, Z. Sheng, H. Han, M. Zou and C. Li, *Mater. Lett.*, 2012, **66**, 222–224.
39 S. A. A. Vandarkuzhali, S. Natarajan, S. Jeyabalan, G. Sivaraman, S. Singaravadivel, S. Muthusubramanian and B. Viswanathan, *ACS Omega*, 2018, **3**, 12584–12592.
40 A. Prasannan and T. Imae, *Ind. Eng. Chem. Res.*, 2013, **52**, 15673–15678.
41 W. Lu, X. Qin, S. Liu, G. Chang, Y. Zhang, Y. Luo, A. M. Asiri, A. O. Al-Youbi and X. Sun, *Anal. Chem.*, 2012, **84**, 5351–5357.
42 L. Zhu, Y. Yin, C. Wang and S. Chen, *J. Mater. Chem. C*, 2013, **1**, 4925–4932.
43 Y. Wang, Z. Shi and J. Yin, *ACS Appl. Mater. Interfaces*, 2011, **3**, 1127–1133.
44 D. Gu, S. Shang, Q. Yu and S. Jie, *Appl. Surf. Sci.*, 2016, **390**, 38–42.
45 Y. Feng, D. Zhong, H. Miao and X. Yang, *Talanta*, 2015, **140**, 128–133.
46 A. Alam, B. Park, Z. Ghouri, M. Park and K. Hak Yong, *Green Chem.*, 2015, **17**, 3791–3797.
47 J. Shen, S. Shang, X. Chen, D. Wang and Y. Cai, *Mater. Sci. Eng., C*, 2017, **76**, 856–864.
48 W. Liu, C. Li, X. Sun, W. Pan, G. Yu and J. Wang, *Nanotechnology*, 2017, **28**, 485705.
49 T. Pal, S. Mohiyuddin and G. Packirisamy, *ACS Omega*, 2018, **3**, 831–843.
50 J. Wang, Y. Hwee Ng, Y. Lim and G. W. Ho, *RSC Adv.*, 2014, **4**, 44117–44123.
51 H. Peng and J. Travas-Sejdic, *Chem. Mater.*, 2009, **21**, 5563–5565.
52 H. Zhu, X. Wang, Y. Li, Z. Wang, F. Yang and X. Yang, *Chem. Commun.*, 2009, 5118–5120.
53 L. Tang, R. Ji, X. Cao, J. Lin, H. Jiang, X. Li, K. S. Teng, C. M. Luk, S. Zeng, J. Hao and S. P. Lau, *ACS Nano*, 2012, **6**, 5102–5110.
54 B. Shi, Y. Su, L. Zhang, M. Huang, R. Liu and S. Zhao, *ACS Appl. Mater. Interfaces*, 2016, **8**, 10717–10725.
55 X. Gong, Q. Zhang, Y. Gao, S. Shuang, M. M. F. Choi and C. Dong, *ACS Appl. Mater. Interfaces*, 2016, **8**, 11288–11297.
56 S. Cailotto, E. Amadio, M. Facchin, M. Selva, E. Pontoglio, F. Rizzolio, P. Riello, G. Toffoli, A. Benedetti and A. Perosa, *ACS Med. Chem. Lett.*, 2018, **9**, 832–837.
57 M. Shehab, S. Ebrahim and M. Soliman, *J. Lumin.*, 2017, **184**, 110–116.
58 Y. Li, X. Zhong, A. E. Rider, S. A. Furman and K. Ostrikov, *Green Chem.*, 2014, **16**, 2566–2570.
59 V. Gude, A. Das, T. Chatterjee and P. K. Mandal, *Phys. Chem. Chem. Phys.*, 2016, **18**, 28274–28280.
60 S. Hill, D. Benito-Alifonso, D. J. morgan, S. A. Davis, M. Berry and M. C. Galan, *Nanoscale*, 2016, **8**, 18630–18634.
61 C. Liu, P. Zhang, F. Tian, W. Li, F. Li and W. Liu, *J. Mater. Chem.*, 2011, **21**, 13163–13167.

62 D. Kim, Y. Choi, E. Shin, Y. K. Jung and B. Kim, *RSC Adv.*, 2014, **4**, 23210–23213.
63 Y. A. Shchipunov, O. N. Khlebnikov and V. E. Silant'ev, *Polym. Sci., Ser. B*, 2015, **57**, 16–22.
64 D. Chowdhury, N. Gogoi and G. Majumdar, *RSC Adv.*, 2012, **2**, 12156–12159.
65 S. Chandra, S. H. Pathan, S. Mitra, B. H. Modha, A. Goswamic and P. Pramanik, *RSC Adv.*, 2012, **2**, 3602–3606.
66 P. Shen, J. Gao, J. Cong, Z. Liu, C. Li and J. Yao, *ChemistrySelect*, 2016, **1**, 1314–1317.
67 M. Hu, Y. Yang, X. Gu, Y. Hu, J. Huang and C. Wang, *RSC Adv.*, 2014, **4**, 62446–62452.
68 C. Yang, P. R. Thomsen, R. Ogaki, J. Kjems and B. M. Teo, *J. Mater. Chem. B*, 2015, **3**, 4577–5484.
69 M. Zhang, Z. Fang, X. Zhao, Y. Niu, J. Lou, L. Zhao, Y. Wu, S. Zou, F. Du and Q. Shao, *RSC Adv.*, 2016, **6**, 104979–104984.
70 J. Jiang, Y. He, S. Li and H. Cui, *Chem. Commun.*, 2012, **48**, 9634–9636.
71 H. Huang, C. Li, S. Zhu, H. Wang, C. Chen, Z. Wang, T. Bai, Z. Shi and S. Feng, *Langmuir*, 2014, **30**, 13542–13548.
72 H. V. Xu, X. Zheng, Y. Zhao and Y. N. Tan, *ACS Appl. Mater. Interfaces*, 2018, **10**, 19881–19888.
73 Y. Zeng, D. n. Maa, W. Wang, J. Chen, L. Zhou, Y. Zheng, K. Yub and S. Huang, *Appl. Surf. Sci.*, 2015, **342**, 136–143.
74 M. Zheng, S. Ruan, S. Liu, T. Sun, D. Qu, H. Zhao, Z. Xie, H. Gao, X. Jing and Z. Sun, *ACS Nano*, 2015, **9**, 11455–11461.
75 P. Karfa, E. Roy, S. Patra, S. Kumar, A. Tarafdar, R. Madhuri and P. K. Sharma, *RSC Adv.*, 2015, **5**, 58141–58153.
76 E. Arad, S. K. Bhunia, J. Jopp, S. Kolusheva, H. Rapaport and R. Jelinek, *Adv. Therap.*, 2018, 1800006.
77 Y. Jiang, Q. Han, C. Jin, J. Zhang and B. Wang, *Mater. Lett.*, 2015, **141**, 366–368.
78 Z. Wang, Y. Qu, X. Gao, C. Mu, J. Bai and Q. Pu, *Mater. Lett.*, 2014, **129**, 122–125.
79 X. Wu, F. Tian, W. Wang, J. Chen, M. Wu and J. X. Zhao, *J. Mater. Chem. C*, 2013, **1**, 4676–4684.
80 L. Li, L. Li, C. Wang, K. Liu, R. Zhu, H. Qiang and Y. Lin, *Microchim. Acta*, 2015, **182**, 763–770.
81 Z. Zhang, J. Hao, J. Zhang, B. Zhang and J. Tang, *RSC Adv.*, 2012, **2**, 8599–8601.
82 Q. Yang, L. Wei, X. Zheng and L. Xiao, *Sci. Rep.*, 2015, **5**, 17727.
83 X. Liu, T. Li, Y. Hou, Q. Wu, J. Yi and G. Zhang, *RSC Adv.*, 2016, **6**, 11711–11718.
84 A. Gedanken, V. B. Kumar, Y. Sheinberger, Z. I. Porat and Y. Shav-Tal, *J. Mater. Chem. B*, 2016, **4**, 2913–2920.
85 M. Tan, X. Li, H. W. Beibei and W. Jing, *Colloids Surf., B*, 2015, **136**, 141–149.
86 Q. Wang, X. Huang, Y. Long, X. Wang, H. Zhang, R. Zhu, L. Liang, P. Teng and H. Zheng, *Carbon*, 2013, **59**, 192–199.
87 L. Sai, J. Chen, Q. Chang, W. Shi, Q. Chen and L. Huang, *RSC Adv.*, 2017, **7**, 16608–16615.
88 D. Chakraborty, S. Sarkar and P. K. Das, *ACS Sustainable Chem. Eng.*, 2018, **6**, 4661–4670.
89 Q. Liang, W. Ma, Y. Shi, Z. Li and X. Yang, *Carbon*, 2013, **60**, 421–428.
90 https://en.wikipedia.org/wiki/Nucleic_acid.
91 C. X. Guo, J. Xie, B. Wang, X. Zheng, H. B. Yang and C. M. Li, *Sci. Rep.*, 2013, **3**, 2957.
92 Q. Li, L. Zhang, J. Bai, Z. Liu, R. Liang and J. Qiu, *Biosens. Bioelectron.*, 2015, **74**, 886–894.
93 T. Song, X. Zhu, S. Zhou, G. Yang, W. Gan and Q. Yuan, *Appl. Surf. Sci.*, 2015, **347**, 505–513.
94 H. Ding, F. Du, P. Liu, Z. Chen and J. Shen, *ACS Appl. Mater. Interfaces*, 2015, **7**, 6889–6897.
95 S. Venkateswarlu, B. Viswanath, A. S. Reddy and M. Yoon, *Sens. Actuators, B*, 2018, **258**, 172–183.
96 K. Yang, M. Liu, Y. Wang, S. Wang, H. Miao, L. Yang and X. Yang, *Sens. Actuators, B*, 2017, **251**, 503–508.
97 X. Hua, Y. Bao, H. Wang, Z. Chen and F. Wu, *Nanoscale*, 2017, **9**, 2150–2161.
98 H. U. Lee, S. Y. Park, E. S. Park, B. Son, S. C. Lee, J. W. Lee, Y. Lee, K. S. Kang, M. Kim, H. G. Park, S. Choi, Y. S. Huh, S. Lee, K. Lee, Y. Oh and J. Lee, *Sci. Rep.*, 2014, **4**, 4665.
99 F. Lin, C. Li and Z. Chen, *Front. Microbiol.*, 2018, **9**, 259.
100 Z. Wang, J. Yu, X. Zhang, N. Li, B. Liu, Y. Li, Y. Wang, W. Wang, Y. Li, L. Zhang, S. Dissanayake, S. L. Suib and L. Sun, *ACS Appl. Mater. Interfaces*, 2016, **8**, 1434–1439.
101 G. Huang, X. Chen, C. Wang, H. Zheng, Z. Huang, D. Chen and H. i. Xie, *RSC Adv.*, 2017, **7**, 47840–47847.
102 F. Du, M. Zhang, X. Li, J. Li, X. Jiang, Z. Li, Y. Hua, G. Shao, J. Jin, Q. Shao, M. Zhou and A. Gong, *Nanotechnology*, 2014, **25**, 315702.
103 S. S. Jones, P. Sahatiya and S. Badhulika, *New J. Chem.*, 2017, **41**, 13130–13139.
104 P. Hsu, Z. Shih, C. Lee and H. Chang, *Green Chem.*, 2012, **14**, 917–920.
105 S. Liu, J. Tian, L. Wang, Y. Zhang, X. Qin, Y. Luo, A. M. Asiri, A. O. Al-Youbi and X. Sun, *Adv. Mater.*, 2012, **24**, 2037–2041.
106 A. B. Suryawanshi, M. Biswal, D. S. Mhamane, R. R. Gokhale, S. Patil, D. Guin and S. Ogale, *Nanoscale*, 2014, **6**, 11664–11670.
107 N. R. Nirala, G. Khandelwal, B. Kumar, V. Rajiv Prakash and V. Kumar, *Talanta*, 2017, **173**, 36–43.
108 J. Feng, W. Wang, X. Hai, Y. Yu and J. Wang, *J. Mater. Chem. B*, 2016, **4**, 387–393.
109 D. Sun, R. Ban, P. Zhang, G. Wu, J. Zhang and J. Zhu, *Carbon*, 2013, **64**, 624–634.
110 C. E. S. Barbosa, J. R. Correa, G. A. Medeiros, G. Barreto, K. G. Magalh, A. L. Oliveira, J. Spencer, M. O. Rodrigues and B. A. D. Neto, *Chem.–Eur. J.*, 2015, **21**, 5055–5060.
111 R. Liu, J. Zhang, M. Gao, Z. Li, J. Chen, D. Wu and P. Liu, *RSC Adv.*, 2015, **5**, 4428.
112 J. Essner, C. H. Laber, S. Ravula, L. Polo-Parada and G. A. Baker, *Green Chem.*, 2016, **18**, 243–250.
113 M. P. Sk, A. Jaiswal, A. Paul, S. S. Ghosh and A. Chattopadhyay, *Sci. Rep.*, 2012, **2**, 383.
114 J. Wang, C. Wang and S. Chen, *Angew. Chem., Int. Ed.*, 2012, **51**, 1–6.
115 S. Mahesh, C. L. Lekshmi, K. D. Renuka and K. Joseph, *Part. Part. Syst. Charact.*, 2016, **33**, 70–74.
116 J. Wang, S. Sahu, S. K. Sonkar, K. N. Tackett, K. W. Sun, Y. Liu, H. Maimaiti, P. Anilkumar and Y. Sun, *RSC Adv.*, 2013, **3**, 15604–15607.

117 Z. Wang, H. Liao, H. Wu, B. Wang, H. Zhao and M. Tan, *Anal. Methods*, 2015, **7**, 8911–8917.
118 S. Han, H. Zhang, J. Zhang, Y. Xie, L. Liu, H. Wang, X. Li, W. Liu and Y. Tang, *RSC Adv.*, 2014, **4**, 58084–58089.
119 Y. Zhou, Y. Liu, Y. Li, Z. He, Q. Xu, Y. Chen, J. Street, H. Guo and M. Nelles, *RSC Adv.*, 2018, **8**, 23657–23662.
120 Z. Ding, F. Li, J. Wen, X. Wang and R. Sun, *Green Chem.*, 2018, **20**, 1383–1390.
121 J. Wei, J. Shen, X. Zhang, S. Guo, J. Pan, X. Hou, H. Zhang, L. Wang and B. Feng, *RSC Adv.*, 2013, **3**, 13119–13122.
122 W. Wang, C. Damm, J. Walter, T. J. Nacken and W. Peukert, *Phys. Chem. Chem. Phys.*, 2016, **18**, 466–475.
123 W. Wang, B. Wang, H. Embrechts, C. Damm, A. Cadranel, V. Strauss, M. Distaso, V. Hinterberger, D. M. Guldi and W. Peukert, *RSC Adv.*, 2017, **7**, 24771–24780.
124 V. Strauss, A. Kahnt, E. M. Zolnhofer, K. Meyer, H. Maid, C. Placht, W. Bauer, T. J. Nacken, W. Peukert, S. H. Etschel, M. Halik and D. M. Guldi, *Adv. Funct. Mater.*, 2016, **26**, 7975–7985.
125 V. Strauss, J. T Margraf, C. Dolle, B. Butz, T. J. Nacken, J. Walter, W. Bauer, W. Peukert, E. Spiecker, T. Clark and D. M. Guldi, *J. Am. Chem. Soc.*, 2014, **136**, 17308–17316.
126 V. Straussa, J. T. Margrafa, T. Clark and D. M. Guldi, *Chem. Sci.*, 2015, **6**, 6878–6885.
127 H. Nie, M. Li, Q. Li, S. Liang, Y. Tan, L. Sheng, W. Shi and S. X.-A. Zhang, *Chem. Mater.*, 2014, **26**, 3104–3112.
128 H. Ding, S.-B. Yu, J.-S. Wei and H.-M. Xiong, *ACS Nano*, 2016, **10**, 484–491.
129 X. Tan, Y. Li, X. Li, S. Zhou, L. Fan and S. Yang, *Chem. Commun.*, 2015, **51**, 2544–2546.
130 S. Yang, J. Sun, P. He, X. Deng, Z. Wang, C. Hu, G. Ding and X. Xie, *Chem. Mater.*, 2015, **27**, 2004–2011.
131 L. Zheng, Y. Chi, Y. Dong, J. Lin and B. Wang, *J. Am. Chem. Soc.*, 2009, **131**, 4564–4565.
132 S. Roy, S. Pramanik, S. Bhandari and A. Chattopadhyay, *Langmuir*, 2017, **33**, 14627–14633.
133 S. Pramanik, S. Bhandari and A. Chattopadhyay, *J. Mater. Chem. C*, 2017, **5**, 7291–7296.
134 S. Bhandari, S. Pramanik, R. Khandelia and A. Chattopadhyay, *ACS Appl. Mater. Interfaces*, 2016, **8**, 1600–1605.
135 S. Pramanik, S. Bhandari, S. Roy and A. Chattopadhyay, *J. Phys. Chem. Lett.*, 2015, **6**, 1270–1274.
136 M. K. Barman, B. Paramanik, D. Bain and A. Patra, *Chem.–Eur. J.*, 2016, **22**, 1–8.
137 T. H. Kim, A. R. White, J. P. Sirdaarta, W. Ji, I. E. Cock, J. John, S. Boyd, C. L. Brown and Q. Li, *ACS Appl. Mater. Interfaces*, 2016, **8**, 33102–33111.
138 S. Qu, D. Zhou, D. Li, W. Ji, P. Jing, D. Han, L. Liu, H. Zeng and D. Shen, *Adv. Mater.*, 2016, **28**, 3516–3521.
139 Y. Wang, K. Wang, Z. Han, Z. Yin, C. Zhou, F. Du, S. Zhou, P. Chen and Z. Xie, *J. Mater. Chem. C*, 2017, **5**, 9629–9637.
140 P. Dong, B. Jiang, W. Liang, Y. Huang, Z. Shib and X. Shen, *Inorg. Chem. Front.*, 2017, **4**, 712–718.
141 R. Sekiya, Y. Uemura, H. Murakami and T. Haino, *Angew. Chem., Int. Ed.*, 2014, **53**, 1–6.
142 X. Feng, F. Zhang, Y. Wang, Y. Zhang, Y. Yang and X. Liu, *J. Electron. Mater.*, 2016, **45**, 2784–2788.
143 S. Mandani, B. Sharma, D. Dey and T. K. Sarma, *RSC Adv.*, 2016, **6**, 84599–84603.
144 N. Papaioannou, A. Marinovic, N. Yoshizawa, A. E. Goode, M. Fay, A. Khlobystov, M. Titirici and A. Sapelkin, *Sci. Rep.*, 2018, **8**, 6559.
145 P. Roy, A. P. Periasamy, C. Chuang, Y. Liou, Y. Chen, J. Joly, C. Liang and H. Chang, *New J. Chem.*, 2014, **38**, 4946–4951.
146 S. Lu, R. Cong, S. Zhu, X. Zhao, J. Liu, J. S. Tse, S. Meng and B. Yang, *ACS Appl. Mater. Interfaces*, 2016, **8**, 4062–4068.
147 X. Shen, B. Sun, D. Liu and S.-T. Lee, *J. Am. Chem. Soc.*, 2011, **133**, 19408–19415.
148 J. Briscoe, A. Marinovic, M. Sevilla, S. Dunn and M. Titirici, *Angew. Chem., Int. Ed.*, 2015, **54**, 4463–4468.
149 L. Bao, Z.-L. Zhang, Z.-Q. Tian, L. Zhang, C. Liu, Y. Lin, B. Qi and D.-W. Pang, *Adv. Mater.*, 2011, **23**, 5801–5806.
150 I. Mihalache, A. Radoi, M. Mihaila, C. Munteanu, A. Marin, M. Danila, M. Kusko and C. Kusko, *Electrochim. Acta*, 2015, **153**, 306–315.
151 X. Fang, M. Li, K. Guo, J. Li, M. Pan, L. Bai, M. Luoshan and X. Zhao, *Electrochim. Acta*, 2014, **137**, 634–638.
152 T. Juang, J. Kao, J. Wang, S. Hsu and C. Chen, *Adv. Mater. Interfaces*, 2018, 1800031.
153 J. Briscoe, A. Marinovic, M. Sevilla, S. Dunn and M. Titirici, *Angew. Chem., Int. Ed.*, 2015, **54**, 1–7.
154 X. Guo, H. Zhang, H. Sun, M. O. Tade and S. Wang, *ChemPhotoChem*, 2017, **1**, 116–119.
155 A. Marinovic, L. S. Kiat, S. Dunn, M. Titirici and J. Briscoe, *ChemSusChem*, 2017, **10**, 1004–1013.
156 Y. Meng, Y. Zhang, W. Sun, M. Wang, B. He, H. Chen and Q. Tang, *Electrochim. Acta*, 2017, **257**, 259–266.
157 G. A. M. Hutton, B. Reuillard, B. C. M. Martindale, C. A. Caputo, C. W. J. Lockwood, J. N. Butt and E. Reisner, *J. Am. Chem. Soc.*, 2016, **138**(51), 16722–16730.
158 A. Pal, G. Natu, K. Ahmad and A. Chattopadhyay, *J. Mater. Chem. A*, 2018, **6**, 4111–4118.
159 B. Martindale, G. A. Hutton, C. A. Caputo, S. Prantl, R. Godin, J. R. Durrant and E. Reisner, *Angew. Chem., Int. Ed.*, 2017, **56**, 6459–6463.
160 X. Wang, J. Cheng, H. Yu and J. Yu, *Dalton Trans.*, 2017, **46**, 6417–6424.
161 J. Qin and H. Zeng, *Appl. Catal., B*, 2017, **209**, 161–173.
162 H. Li, X. Zhang and D. R. MacFarlane, *Adv. Energy Mater.*, 2015, **5**, 1401077.
163 W.-J. Ong, L. K. Putri, Y.-C. Tan, L.-L. Tan, N. Li, Y. H. Ng, X. Wen and S.-P. Chai, *Nano Res.*, 2017, **10**, 1673–1696.
164 Q. Zhang, J. Jie, S. Diao, Z. Shao, Q. Zhang, L. Wang, W. Deng, W. Hu, H. Xia, X. Yuan and S.-T. Lee, *ACS Nano*, 2015, **9**, 1561–1570.
165 C. O. Kim, S. W. Hwang, S. Kim, D. H. Shin, S. S. Kang, J. M. Kim, C. W. Jang, J. H. Kim, K. W. Lee, S.-H. Choi and E. Hwang, *Sci. Rep.*, 2014, **4**, 5603.
166 L. Tang, R. Ji, X. Li, G. Bai, C. P. Liu, J. Hao, J. Lin, H. Jiang, K. S. Teng, Z. Yang and S. P. Lau, *ACS Nano*, 2014, **8**, 6312–6320.

